

Alma Mater Studiorum – Università di Bologna

DOTTORATO DI RICERCA IN

Scienze degli Alimenti, Nutrizione animale e sicurezza alimentare-SANASA
Ciclo XXV

Settore Concorsuale di afferenza: 06/D4

Settore Scientifico disciplinare: MED12

TITOLO TESI

**SVILUPPO DI NUOVI APPROCCI TERAPEUTICI NELLE MALATTIE
INFIAMMATORIE CRONICHE INTESTINALI: CIBI FUNZIONALI E
NUTRACEUTICI VS VACCINI A BASE DI PEPTIDI SINTETICI**

Presentata da: GIULIA RODA

Coordinatore Dottorato

Prof. Roberto Rosmini

Relatore

Dr. Mara Mirasoli

Esame finale anno 2013

TITLE

DEVELOPMENT OF NEW THERAPEUTICAL APPROACHES IN THE
TREATMENT OF INFLAMMATORY BOWEL DISEASE: FUNCTIONAL FOOD
AND NUTRACEUTICALS VS SYNTHETIC PEPTIDES BASED VACCINES

INDEX

INTRODUCTION

1. Functional Food and Nutraceuticals in the treatment of Inflammatory Bowel Disease

1.1 Background

1.2 Curcuma longa

1.3 Curcuma and IBD

1.4 Myorelaxant effect of curcuma in a mouse model of colitis.

1.4.1. Background

1.4.2 Methods

1.4.3 Results

- Histological parameters, colon length and DAI
- Spontaneous motility in ileum and colon
- Response to Carbachol and Atropine
- Functional Study in DSS Mice Smooth Muscle

1.4.4 Discussion

1.4.5 References

2. Characterization of the role of CEACAM5 in the intestinal immunoregulation

2.1 Background

2.2 Specific aims

2.3 Methods

2.4 Results

2.5 Conclusions

3. Overlapping peptide library as a tool for the development of synthetic peptides to use as potential therapeutic agents.

3.1 Background

3.2 Methods

3.2.1. CEACAM5 overlapping peptide library

3.2.2 Isolation of human CD8+ T cells

3.2.3 In-Cell Western Blot

3.3 Peptides functionality evaluation: CD8-associated LcK phosphorylation

3.4 Conclusion

INTRODUCTION

Inflammatory Bowel Diseases (IBD) are intestinal chronic relapsing diseases which etiopathogenesis remains uncertain. The two main forms are ulcerative colitis and Crohn's disease (1-3).

Several factors have been involved such as genetic susceptibility, environmental factors such as smoke, diet, sex, immunological factors as well as the microbioma.

Several treatments are available for IBD but none of them satisfy several criteria at the same time such as safety, long-term remission, histopathological healing, and specificity.

We have investigated two different approaches to the treatment of IBD which could lead to new drugs development and new treatment algorithm.

The first part of this thesis is focused on the understanding of the potential role of functional food and nutraceuticals in the treatment of IBD. To do so, we investigated the role of *Curcuma longa* in the treatment of chemical induced colitis in mice model. Since *Curcuma Longa* has been investigated for its anti-inflammatory role related to the TNF α pathway as well investigators have reported few cases of patients with ulcerative colites treated with this herbs, we harbored the hypothesis of a role of *Curcuma Longa* in the treatment of IBD as well as we decided to assess its role in intestinal motility.

The second part of this thesis is based on an immunological approach to develop new drugs to induce suppression in Crohn's disease or to induce mucosa immunity such as in colonrectal tumor. The main idea behind this approach is

that we could manipulate relevant cell-cell interactions using synthetic peptides. We demonstrated the role of the unique interaction between molecules expressed on intestinal epithelial cells such as CD1d and CEACAM5 and on CD8⁺ T cells. In normal condition this interaction has a relevant role for the expansion of the suppressor CD8⁺ T cells. Here, we characterized this interaction, we defined which are the epitope involved in the binding and we attempted to develop synthetic peptides from the N domain of CEACAM5 in order to manipulate it.

1. Functional Food and Nutraceuticals in the treatment of Inflammatory Bowel Disease

1.1 Background

Alternative drug treatment is increasing in developed countries. In undeveloped countries such as India (70%), Ruwanda (70%), Uganda (60%), Tanzania (60%), Benin (80%) and Etiopia (90%) the percentages are high.

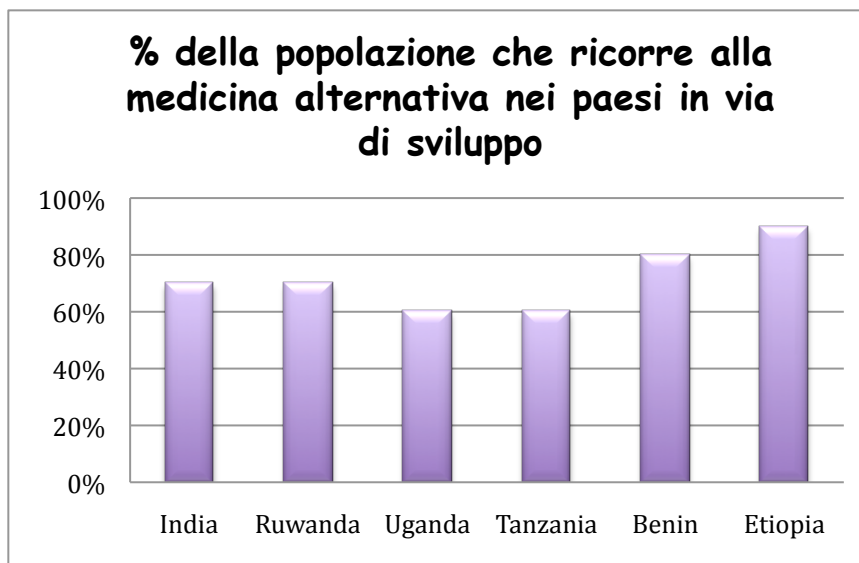


Figure 1. Undeveloped countries

In developed countries such as Belgium (31%), USA (42%), Australia (48%), France (49%), Canada (70%), a significant percentage has used alternative medicine once in their life.

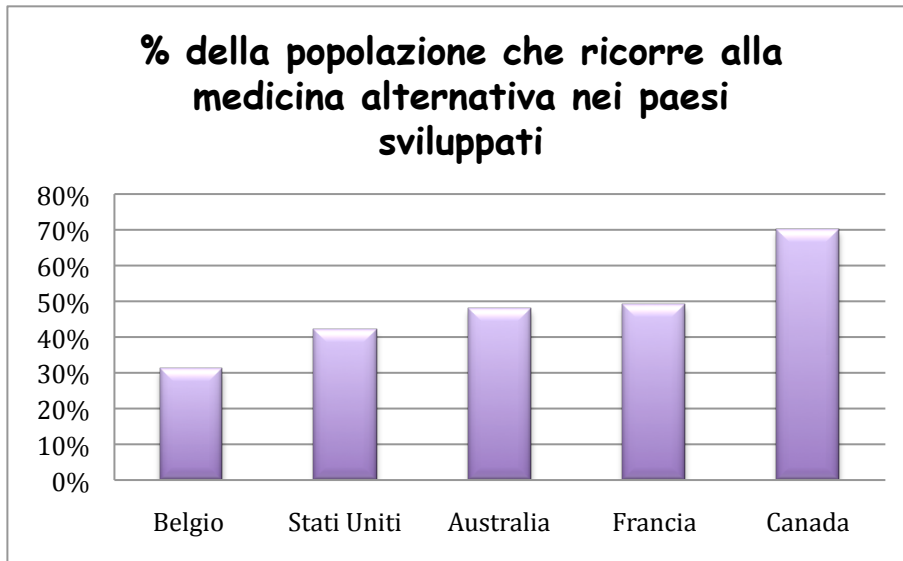


Figure 2. Developed countries

The use of nutraceutical supplements by patients with gastrointestinal disorders is growing worldwide. The literature has shown that there are a discrete number of clinical trials that have demonstrated the efficacy of nutraceutical supplements for IBD such as Probiotics, prebiotics, Curcuma longa, Boswellia serrata, and fish oils.

The main idea behind the use of nutraceuticals in IBD is the characteristics of these products. Several groups have shown their role in modulating inflammatory mediators involved in the inflammatory process, altering luminal bacteria, modifying the immune response, and rejuvenation of intestinal healing.

1.2 Curcuma Longa

Curcuma Longa (turmeric) is a perennial herb, cultivated in the Southeast Asia. Turmeric chemicals include curcumin, demethoxycurcumin, and bisdemethoxycurcumin, as well as volatile oils, sugars, proteins, and resins curcumin being the most studied compounds. Different groups have revealed that curcumin has a wide range of beneficial properties including anti-inflammatory activity, antioxidant, chemotherapeutic and chemopreventive, antimicrobial (4-20). It has been shown that turmeric also possesses a pronounced AchE activity-inhibitory. These studies have paved the way for human clinical trials. Due to its long history as a drug, and because patients show a preference for natural remedies and for their excellent safety profile shown so far, there is, therefore, a discrete number of researchers interested in the use of curcumin for therapeutic purposes.

Its anti-inflammatory and antioxidant effects have been shown in cancer, cardiovascular disease as well as diabetes, atherosclerosis, oxidation of LDL, myocardial infarction and IBD. It has been reported that it inhibits the following biochemical mechanisms: Activating protein-1 (AP-1), Nuclear factor-kappa B (NF- κ B), 1.2-cyclooxygenase (COX1 and COX2) and lipoxygenase (LOX), TNF- α (tumor necrosis factor α), IFN- γ (interferon- γ) and other such as Profiles of adhesion molecules and chemokines, INOS (inducible nitric oxide synthase), Oxidation of glutathione (GSH).

The anti-inflammatory activity may be due to the action of the peroxide radicals

scavenging developed by xanthine and xanthine oxidase. In fact, the anti-inflammatory effect of turmeric has been demonstrated both on edema induced by carrageenan in the rat paw (acute inflammation), both in models of chronic inflammation. Turmeric has the ability to inhibit the peroxidation of lipids liposome and the damage on DNA induced by peroxide; at low concentrations, also was effective in protecting the hepatocytes of the rat by the lipid peroxidation induced by paracetamol. Other studies confirm the antioxidant properties through modulation of glutathione levels.

One of the most important activities for IBD derives from the effect of curcumin on the TNF α pathway. Curcumin blocks the activation of NF- κ B. Different studies have focused the attention on the role of Curcumin administration in the prevention of the development of colitis in experimental mice model. It has been shown that it prevents the Trinitrobenzene Sulfonic Acid (TNBS)-induced colitis inhibiting AP-1, Kinase C and NF- κ B and the colitis in chemical induced Dextran Sodium Sulphate (DSS) model.

Dendritic cells represent a target of Curcumin since blocking of MAPKs and NF- κ B activation has been described.

Curcumin has also been shown able to block significantly the proliferation of spleen lymphocytes induced interleukin 2 and irreversibly inhibit the expression / production of interleukin 2 and interferon- γ by splenic lymphocytes and peritoneal macrophages.

Curcuma longa has potential anticancer remedies. It inhibits the development

and progression of the tumor (Hatcher, 2008) (Figure 3).

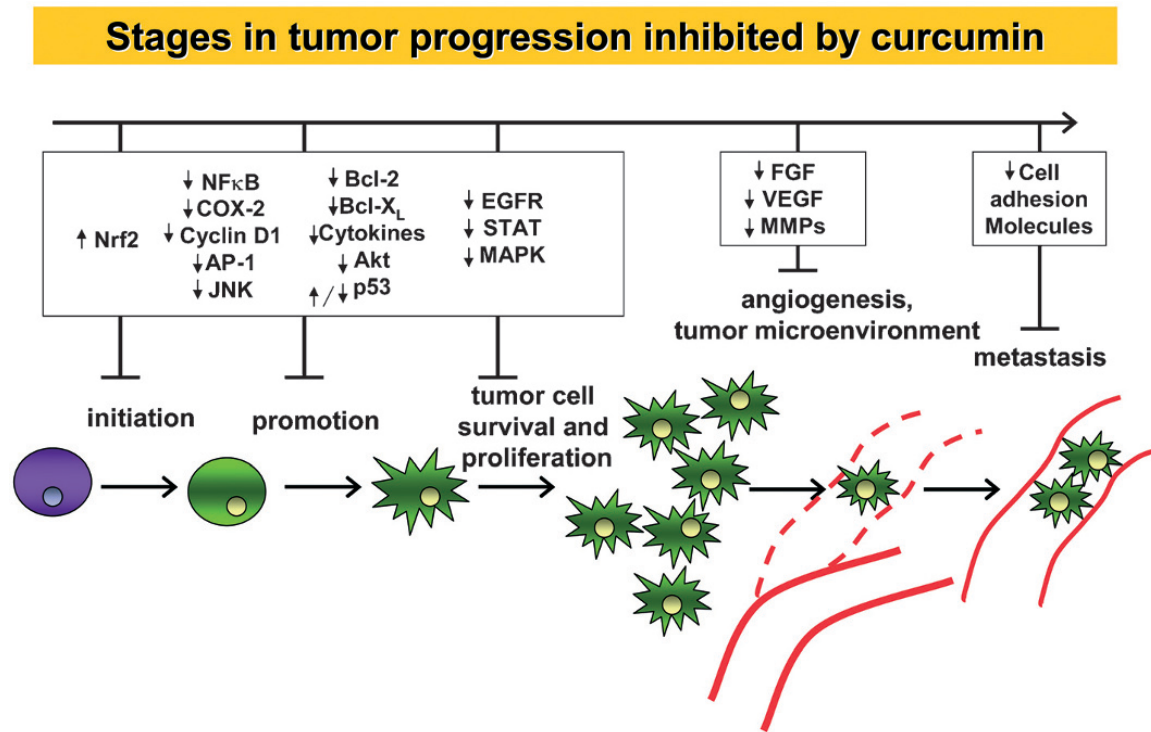


Figure 3. Stages of tumor progression inhibited by turmeric.

Curcuma inhibits the stage of initiation of cancer by preventing activation of the carcinogen and inhibits the proliferation of malignant cells during promotion and progression. Several studies have demonstrated the ability of curcumin to reduce the incidence of tumors induced by benzo (a) pyrene and 7.12 dimethyl benz (a) anthracene and the tumor promoting phorbol ester-induced mouse skin.

Other studies have shown that curcumin inhibits the development of stomach cancer induced by N-methyl-N-nitro-N-nitrosoguanina (MNNG); in rats reduces the incidence and / or the multiplicity of esophageal tumors and preneoplastic lesions induced from N-nitrosometilbenzilamina. The diet of turmeric has significantly reduced the azoximetano-induced preneoplastic lesions in the incidence and / or the multiplicity of tumors at the level of the colon.

Curcumin seems to act simultaneously inhibiting angiogenesis, inducing apoptosis, or more generally the cell death, and acting directly and indirectly (metabolism carcinogens) on carcinogens.

1.3 Curcuma and IBD

Several group have studied the role of curcuma in experimental mice model of colitis. Sugimoto group shown amelioration of colitis in mice with TNBS-induced colitis treated with 0.5%, 2.0% or 5.0% of curcumin (added to their diet). Curcuma suppresses infiltration of effector T cells CD4 (+) and the activation of NF-kB in the colonic mucosa. It also suppresses the formation of proinflammatory cytokines in the colonic mucosa (21). Ukil demonstrates the protective role of curcuma in mice which developed a model IBD characterized by oxidative and nitrosative stress, by infiltration of leukocytes and 'upregulation' of proinflammatory cytokines that are commonly observed in human IBD (22).

Salh group has found that when curcumin is administered before the induction of colitis it reduces the activation of NF-kB (23).

Moreover, it has been observed that administration of curcumin to mice with TNBS induced colitis, prior to induction of colitis, is associated with a marked reduction of the expression of Th1 cytokines (IL-12, IFN- γ , TNF- α , IL-1) and to an increased expression of Th2 cytokines (IL-4 and IL-10) in the colonic mucosa.

Few groups have attempted to study the role of Curcuma in IBD patients (24).

In the pilot study of Holt, curcuma was administered in five patients with ulcerative colitis and five with Crohn's disease. Each patient was administered orally 360 mg of curcumin three times a day for a month and then four times a day for two months. Of the 10 patients, 9 reported improved. Four of the five patients with ulcerative colitis (UC) were able to reduce or to eliminate their complementary treatments.

In a randomized double-blind multicenter Hanai has given to a total of 89 patients with a form of quiescent UC 1g of curcumin (n = 45) twice a day plus sulfasalazine or mesalamine as conventional drug reference to the treatment of patients with IBD. The remaining patients (n = 44) have, however, received the placebo plus sulfasalazine or mesalamine for six months. During the first six months of therapy, the 43 patients who received curcumin, two (4.65%) had relapse, while eight of the 39 patients (20.51%) in the placebo group (P = 0.040), showed relapse. The study of Hanai is the first multicenter study on curcumin in patients with quiescent IBD that have been proven safe and effective in prolonging the time in which patients may remain in quiescence, suggesting that it would be able to suppress recurrence. The obvious benefits to which this would

lead to avoiding mortality associated with clinical relapse and reduce medical costs.

Therefore, the inhibitory effects on the major inflammatory mechanisms such as COX-2, LOX, TNF- α , IFN- γ , NF- κ B and its unparalleled safety profile, make a bright outlook of curcumin in the treatment of IBD. However, clinical studies are needed-controlled trial in a large cohort of patients to fully evaluate the clinical potential of curcumin.

	Experimental colitis	Results	Mechanism
<i>Sugimoto, et al. [2002]</i>	TNBS	+++	<ul style="list-style-type: none"> ↓NF-κB ↓CD4 (+) T cells ↓Proinflammatory cytokines mRNA
<i>Salh, et al. [2003]</i>	DNB	+	<ul style="list-style-type: none"> ↓NF-κB ↓MAPK p38
<i>Ukil, et al [2003]</i>	TNBS	+++	<ul style="list-style-type: none"> ↓Neutrofilis ↓iNOS ↓NF-κB
<i>Jiang, et al. [2006]</i>	TNBS	+	<ul style="list-style-type: none"> ↓COX-2 ↓MPO
<i>Zhang, et al. [2006]</i>	TNBS	++	<ul style="list-style-type: none"> ↓PPAR γ ↓COX-2 ↓Th 1 cytokines ↑Th 2 cytokines
<i>Venkataramanna, et al. [2007]</i>	DNCB	++	<ul style="list-style-type: none"> ↓NF-κB ↓iNOS

Figure 4: Effect of curcuma in Experimental mice model of colitis (21-25).

1.4 Myorelaxant effect of curcuma in a mouse model of colitis

1.4.1 Background

In patients with Inflammatory Bowel Disease the entire functionality of the ileum and colon is altered even when the disease involves specific intestinal segments. Inflammation is associated with a reduction in the formation of haustra and mixing of the colon with increased propulsive motility. A change in cholinergic and adrenergic system as well non adrenergic non cholinergic system have been described in experimental animals, the underlying mechanisms were disturbances of intracellular calcium signaling and mobility, altered release of norepinephrine, impairment of protease-activated receptor 2, defects relaxation dependent inhibitory neurons in the colon.

The toxicity, intolerance to conventional therapy for IBD or the slow onset of action in addition to a more detailed understanding of the mechanisms that underlie the disease and its debilitating nature have been the main reasons that led to seek treatment safer and more effective.

Curcuma longa (turmeric) is used in Ayurvedic medicine as a hepatoprotective agent and as a remedy for several inflammatory diseases. As already said, in traditional medicine has been used for its anti-tumor properties, antimicrobial, anti-inflammatory and antioxidant.

Curcumin has been shown to be effective in trinitrobenzene sulfonic acid (TNBS) experimental mice model through inhibition of the most important of the inflammatory response in signal transduction such as AP-1, protein kinase C and NF- κ B and, likewise, prevents inflammation in chronic colitis DSS (sodium dodecylsulfate)-induced by blocking the activation of NF- κ B in the mucosa. In addition, turmeric, in a randomized, multicenter, double-blind, compared with placebo, was shown to be safe and effective in maintaining remission of ulcerative colitis.

So far, there are a lot of data on anti-inflammatory properties of turmeric in humans and efficacy in preventing DSS-induced colitis in animals, but little is known of the effect of turmeric on intestinal motility (26-38).

The extensive clinical use of *Curcuma Longa* for the treatment of diarrhea in western countries has led the current research in order to assess whether curcumin exerts a direct effect on the motility of the ileum and colon and whether this effect, if there was is observed, in addition to its anti-inflammatory effect in acute and chronic DSS colitis-induced mice.

1.4.2 Methods

Animals

One hundred thirty male Balb/c mice (8 weeks old, 25–30 g b.w.) (Charles Rivers Laboratories, Calco, LC, Italy) were enrolled: a higher number of animals than required were recruited in order to compensate for the drops out in the course of the experiments, due to the severity of colitis compelling to stop the experiments,

according to the Recommendations of the Ethical Committee of the University of Bologna for Animal Experiments. The animals were kept at constant light/dark cycling and constant room temperature of 22°C. They were fed the usual commercial diet.

5 groups were created. A group of 15 healthy mice was used to evaluate the in vitro effect of Curcuma extract on intestinal motility parameters by antagonism of Carbachol-induced contraction. A second and a third group of animals were subjected to Dextran Sodium Sulphate (DSS) (MP Biomedicals, Solon; OH, USA; m.w. 36.000–50.000). The effect of DSS on the Disease Activity parameters and intestinal motility were evaluated. After colitis induction, Curcuma extract was orally administered (200 mg/kg b.w./day). 14 mice were used as controls and 6 mice were used as Curcuma fed control, after oral administration of Curcuma over seven days. Intestinal histology, spontaneously and Carbachol-induced motility were assessed in each mouse. The effect of Atropine in Carbachol-induced contraction was also studied in order to get more insights into the mechanism of action of Curcuma extract on the ileal and colonic contraction.

Study protocol

The in vitro effect of curcuma was evaluated on isolated mice ileum and distal colon segments. Chronic colitis was induced by oral administration of DSS (2.5%, w/v) in drinking water while the animals were fed the usual commercial diet. At the 52nd day, Curcuma was administered to one group. After colitis induction and after 7, 14, 21 days of either Curcuma extract added diet (200 mg/kg/b.w.) or standard diet administration, 6 mice of each group were sacrificed

and the following parameters were evaluated: colon length, intestinal histology and motility. Acute colitis was induced by addition of DSS (5% w/v) in the drinking water for 7 days. After this period, the mice were randomly allotted to two groups, one group continued the standard usual diet, the other was switched to a diet similar to the previous but added with Curcuma (200 mg/kg b.w.); after 7 days, the animals were sacrificed. 14 mice were studied as controls. 6 mice were fed Curcuma added diet over 7 days and thereafter sacrificed and similarly studied. (Figure 4).

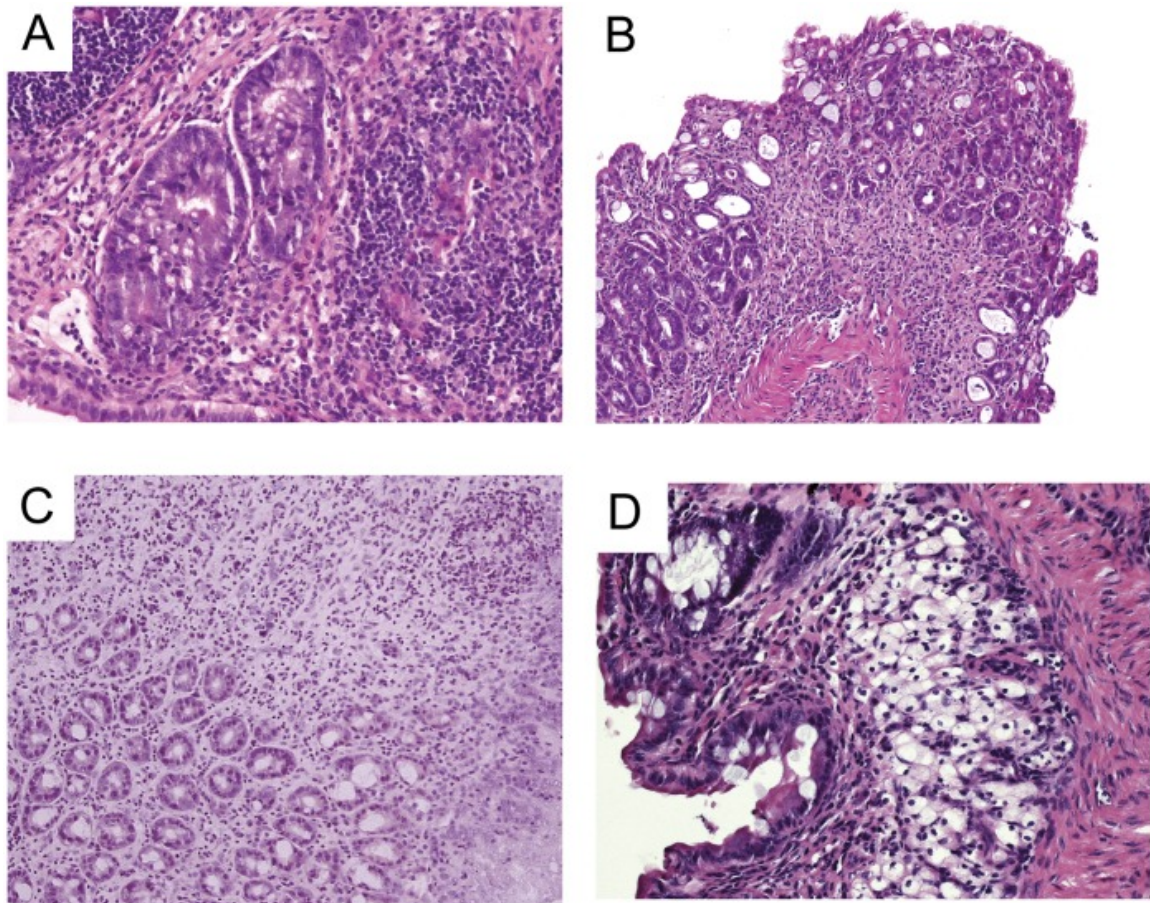


Figure 4

Hematoxylin and eosin staining of Colon sections from DSS (5%w/v over 7 days) treated mice, before (a) and after 7 days Curcuma extract administration (b) and from DSS (2.5%,w/v, three cycles over 52 days) (c) and after 21 days Curcuma

Acute and chronic colitis were induced by DSS administration according to Wirtz group and Disease Activity Index (DAI) was calculated as described by Fitzpatrick. Mice were on a 4RF21diet (Mucedola S.r.l., Milan, Italy). The 4RF21 complete food was added with Curcuma (Indena Spa, Milan, Italy) extract at a final concentration of 1 g/kg. The delivery form of Curcuma used in the present study is a patented formulation of Curcumin (Free Curcumin; Curcuminglucuronide; Curcuminsulphate), a dietary phenolic, with soylecithin. The two compounds form a non-covalent adduct in a 12 weight ratio, and two parts of microcrystalline cellulose are then added to improve formulation. The chemical preparation was proved to be 18–22% pure by HPLC total curcuminoids content.

The day prior to the experiments, food was withdrawn and water was maintained *ad libitum*. The animals were sacrificed by cervical dislocation. A portion of jejunum, immediately after the Treitz was removed (1.5 cm) and retained for histological examination. A 1.5 cm length segment of the terminal ileum, immediately proximal to the ileo-cecal valve and a 2.5 cm region of the distal colon were identified, slightly cleaned with Krebs solution to remove fecal residues and dissected into two parts: one part was placed in 10% formalin for subsequent histological analysis, a second was retained for immediate in vitro motility studies (see below). Stools were analyzed for consistency and blood

traces. The sections of ileum and colon specimens were preserved in 10% neutral buffered formalin for about 48 hours and routinely processed. The histological preparations were examined histologically on a blinded basis. Acute colitis has intense inflammatory cell infiltrate, crypt abscesses, mucin depletion, and surface ulceration, that are the main histological features of acute activity. The hallmark is the presence of neutrophils and eosinophils infiltrating lamina propria and crypt epithelium. Chronic colitis is characterized chronic inflammatory cells, plasma cells and lymphocytes in the lamina propria, distortion of the normal architecture of colonic mucosa, including crypts branching and regeneration. Basal accumulation of lymphocytes and plasma cells with hyperplasia of lymphoid tissue probably represents an early immunologic manifestation of the underlying disease.

Therefore, according to the amount of acute and chronic inflammatory cell infiltrate in colon and in small bowel slides colitis was classified in four grades as reported in Table 1.

TABLE 1: Histological score
0 absence of neutrophils and eosinophils in the lamina propria.
1 Mild and focal infiltrate of neutrophils and eosinophils in the lamina propria with mild crypt aggression.
2 Moderate infiltrate of neutrophils and eosinophils in the lamina propria with moderate crypt aggression.
3 Marked and diffuse infiltrate of neutrophils and eosinophils in the lamina propria with marked crypt aggression.

The animals were sacrificed by cervical dislocation, and the organ (ileum and distal colon) required was set up rapidly under a suitable resting tension in 15 mL organ bath containing appropriate physiological salt solution (PSS) consistent warmed (see below) and buffered to pH 7.4 by saturation with 95% O₂–5% CO₂ gas. The terminal portion of ileum (immediately proximal to the ileo-caecal junction) was cleaned, and segments 1 cm long of ileum were set up under 1 g tension at 37°C in organ baths containing Tyrode solution of the following composition (mM): NaCl, 145; KCl, 2.6; CaCl₂·2H₂O, 1.5; MgCl₂·6H₂O, 0.73; NaH₂PO₄·2H₂O, 0.33; NaHCO₃, 4.8; glucose, 11.1. Each segments was set up under 1 g tension in the longitudinal direction along the intestinal wall. Tissue were allowed to equilibrate for at list 30 min during which time the bathing solution was changed every 10 min. Concentration-response curves were constructed by cumulative addition of the agonist Carbachol (CCh). The concentration of agonist in the organ bath was added only after the response to the previous addition had attained a maximal level and remained steady. Contractions were recorded by means of displacement transducer (FT. 03, Grass Instruments, Quincy, MA) using Power Lab software. Controls not receiving any antagonist were used. Concentration–response curves to agonist were calculated at 30 min intervals, the first one being discarded and the second one used as control. A new concentration-response curve to agonist was obtained following incubation with the antagonist (Atropine or Curcuma extract). Tension changes were recorded isotonicly. A segment of about 2 cm of the distal colon was transected, rinsed with Krebs solution of the following composition (mM):

NaCl, 119; KCl, 4.5; CaCl₂, 2.5; MgSO₄·7H₂O, 2.5; KH₂PO₄·2H₂O, 1.2; NaHCO₃, 25; glucose, 11.1; the mesenteric tissue was removed. The segments were suspended in organ baths containing gassed warm Krebs solution under a load of 1 g maintained at 37°C. Tension changes in longitudinal muscle length were recorded. Tissues were allowed to equilibrate for at least 30 min during which time the bathing solution was changed every 10 min. Concentration–response curves to agonist Carbachol (CCh) were recorded isotonicly and obtained at 30 min intervals, the first one being discarded and the second one taken as control. Following incubation with the antagonists (Atropine or Curcuma extract), a new concentration–response curve to agonist was obtained. Longitudinal muscle contractions were recorded isotonicly by the mean of force displacement transducer (FT 03, Grass Instruments, Quincy, MA) using Power Lab software (ADInstruments Pty Ltd, Castle Hill, Australia). In all cases, parallel experiments in which tissues did not receive any antagonist were run in order to check any variation in sensitivity.

Statistical Analysis

pEC₅₀ values represent the $-\log EC_{50}$. EC₅₀ values are the means \pm SE of at least four independent experiments and were calculated by a non-linear regression curve-fitting computer program.

In functional experiments, dose ratios at the EC₅₀ values of the agonist were calculated at three to five antagonist concentrations, and each concentration was

tested from two to four times. The results are expressed as pA2 values. Data are presented as means \pm SE of n experiments. Differences between mean values were tested for significance by Student's t -test. P value less than 0.05 was considered significant. The antagonism activity to CCh of curcuma extract was estimated by determining the concentration of the non-competitive antagonist that inhibited 50% of the maximum response to the agonist. Three different antagonist concentrations were used and each concentration was tested at least three times. A pharmacological computer program was used to analyze data. It was always verified that EC50 values for the agonist in tissues receiving only the solvent were not significantly different ($P > 0.05$) from control values. In other cases experiments were discarded.

1.4.3 Results

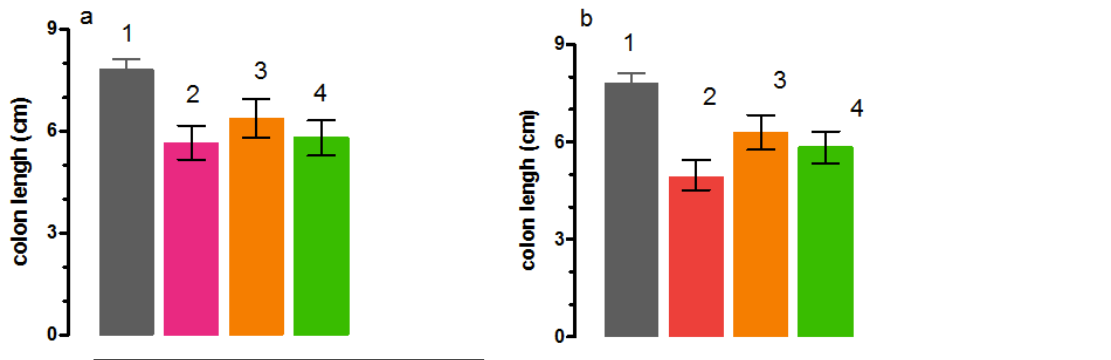
Histological parameters, colon length and DAI

Both the ileum and the distal colon of the control mice demonstrated a very mild lymphocytic infiltration, typical for the “physiological inflammation”.

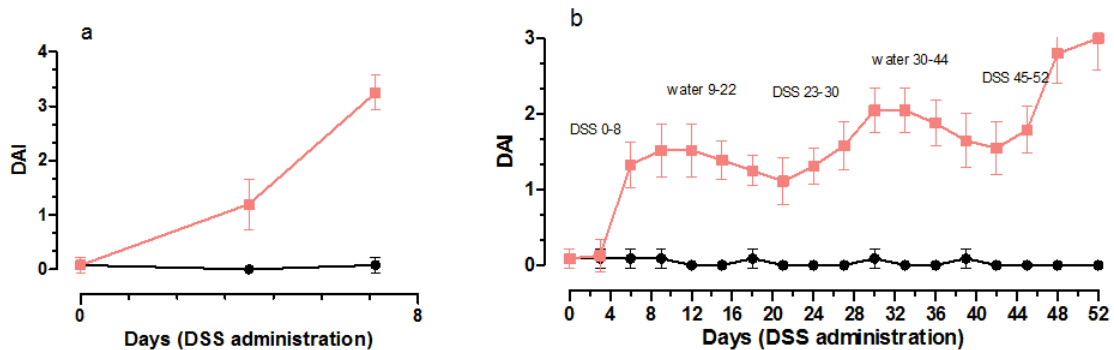
		Histological Grading			
		After colitis induction	After 7 days	After 14 days	After 21 days
Controls		0	0	0	0
Acute colitis	followed by standard diet	3–3	2–3		
	Followed by curcuma extract	3–3	1–2		
Chronic colitis	followed by standard diet	3–3	2–3	2–3	2–2
	followed by curcuma extract	2–3	2–2	1–2	0–1

Severe edema, inflammatory cells infiltration with granulocytes into both the mucosa and the submucosa, with destruction of the epithelial cells are the common features of Acute DSS-induced colitis. One week after discontinuation of DSS, mice assuming Curcuma has a lower histological score.

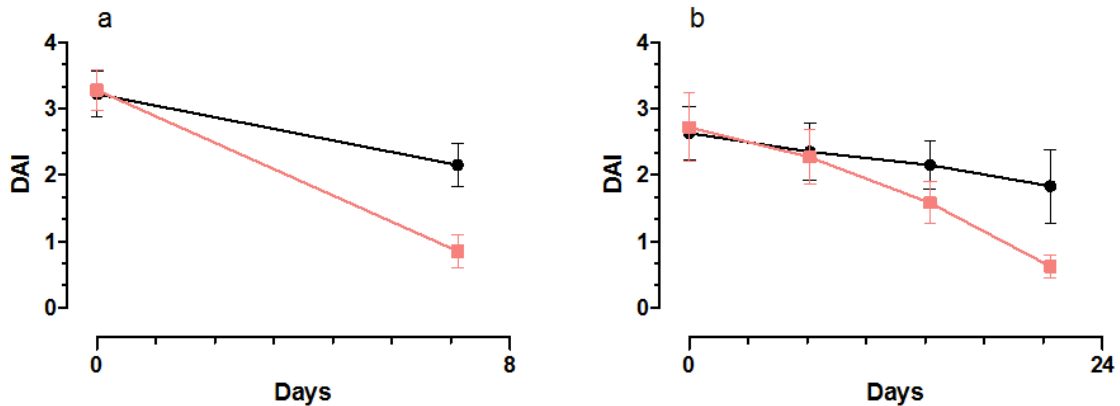
In chronic DSS induced colitis, chronic inflammatory cells sometimes with mild neutrophil infiltrate were present in the mucosa and submucosa. 3 weeks after withdrawal, mice under Curcuma extract had a lower histological score.



Effect of acute (a) and chronic (b) DSS administration on colon length: a1) control. a2) acute colitis. a3) acute colitis treated with curcuma for 7 days. a4) acute colitis + standard diet for 7 days. b1) control. b2) chronic colitis. b3) chronic colitis treated with curcuma extract for 21 days. b4) chronic colitis + standard diet for 21 days.



DAI in the acute (a) and chronic colitis (b) model.



DAI in mice + curcuma (red) or + standard diet (black) after acute (a) and chronic (b) colitis induction.

Spontaneous motility in ileum and colon

The ileal and colonic contractions in basal conditions were used as control. In vitro curcuma extract inhibited the spontaneous intestinal contraction by 100% in ileum and colon (Figure 5). In vivo, when orally administered over one week to control mice, there was a reduction of 30%. In acute model, there was increase of 230% in the ileum and the contractions were highly irregular in amplitude and frequency; colonic contractions were reduced of 100%. One week of Curcuma diet results in 50% of reduction in the ileum, while standard diet did not affect contractions. In chronic DSS colitis, spontaneous contractions increased by 400% and 300% respectively in the ileum and colon. They were of irregular amplitude and frequency. Seven days after curcuma administration, a partial normalization was observed in both the ileum and the colon; 14 days after Curcuma administration the basal ileal and colonic motility were normalized and were of constant amplitude and frequency. A longer administration (21 days)

inhibited the basal spontaneous activity of the ileum and colon.

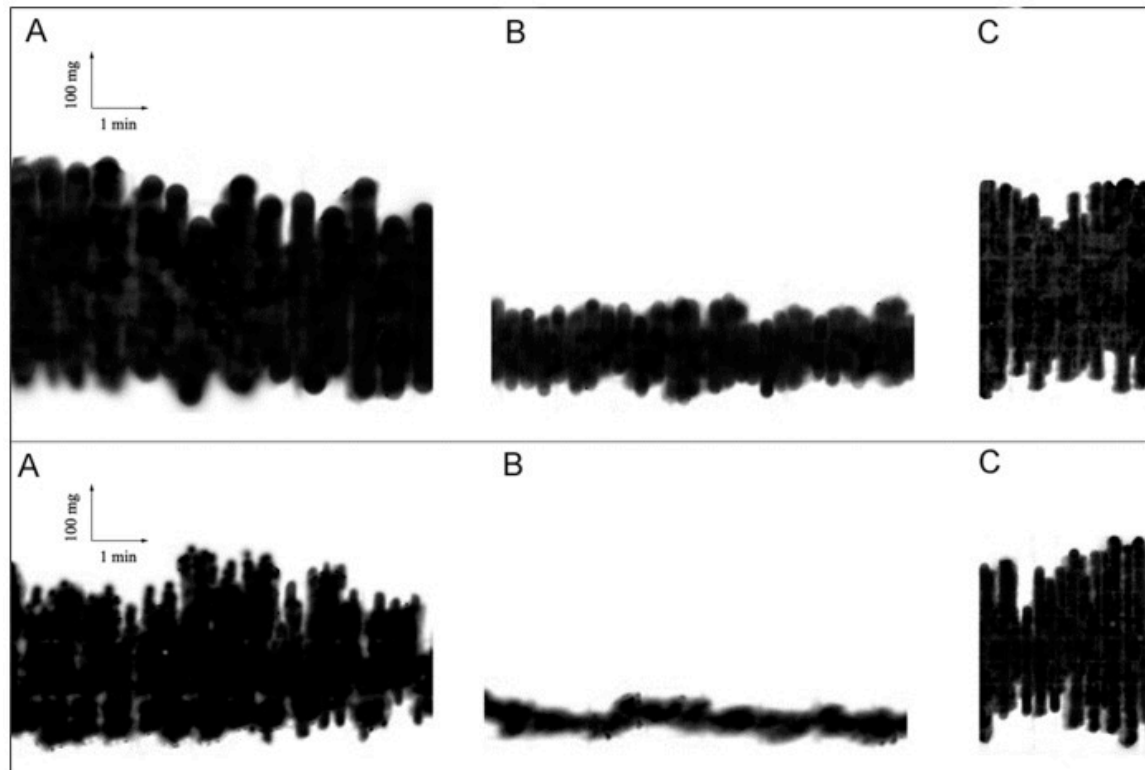


Figure 5. Inhibition of spontaneous motility of ileum (upper panel) and colon (lower panel) by curcuma extract. In control conditions (a), after curcuma extract (b) and after washing (c).

Response to Carbachol and Atropine

Experiments performed in mice ileum and colon showed that Curcuma extract inhibited the maximum response to Carbachol in a non-competitive manner. These results show that the extract produce a smooth muscle relaxation effect on mice ileum and colon. Furthermore, this blockade was reversed after 30 min tissue washing (Figure 6). The IC₅₀ value for Curcuma extract was 0.03 mg/ml in ileum and 0.04 mg/min distal colon respectively. In both cases, the agonist

activity was comparable. In order to evaluate the effects of Curcuma extract on the intestinal muscular layers of ileum and colon, we have used as reference the contraction induced by Carbachol and the antagonistic effects of Atropine. Figure 4 reports Carbachol pEC50 and Atropine pA2 on ileum and colon respectively.

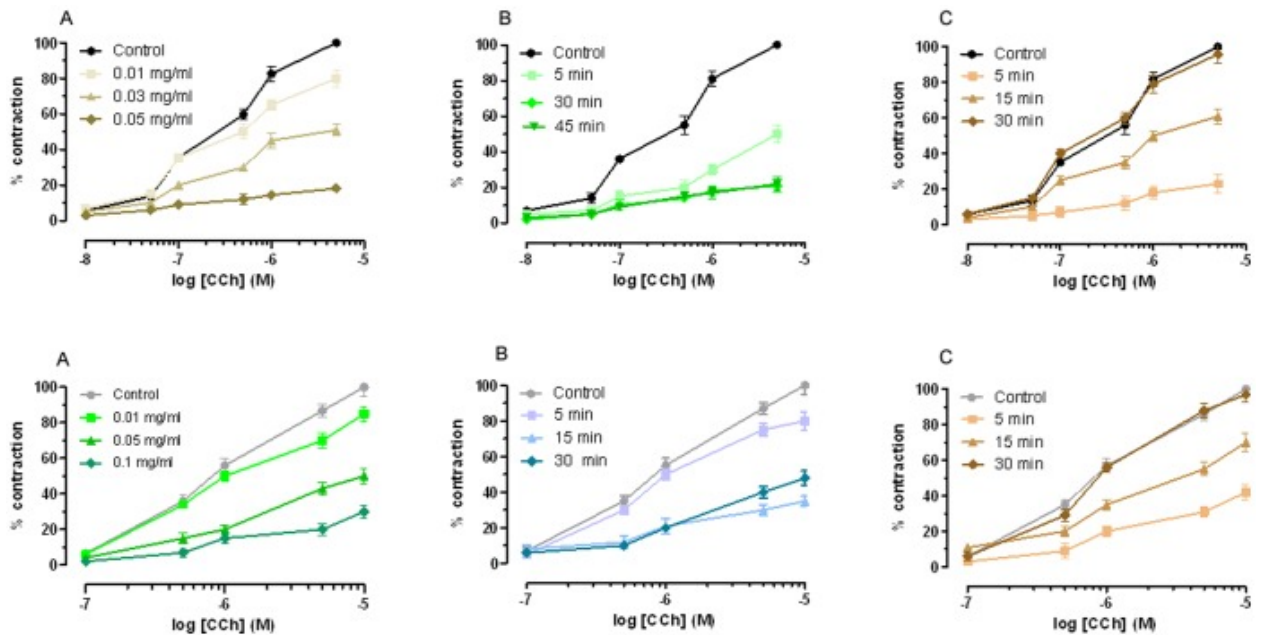


Figure 6

Carbachol results more potent on the ileum than on the colon. Atropine has similar antagonistic activity on both tissues: these data have been used as a comparison with the effect of Carbachol and Atropine on tissues from DSS treated animals (acute and chronic colitis) and after Curcuma extract or placebo administration.

Functional Study in DSS Mice Smooth Muscle

Acute colitis

Carbachol induced contraction was reduced: in the ileum Charbacol pEC50 decreased by 3.80 times and in the colon by 1.58 times (Figure 7).

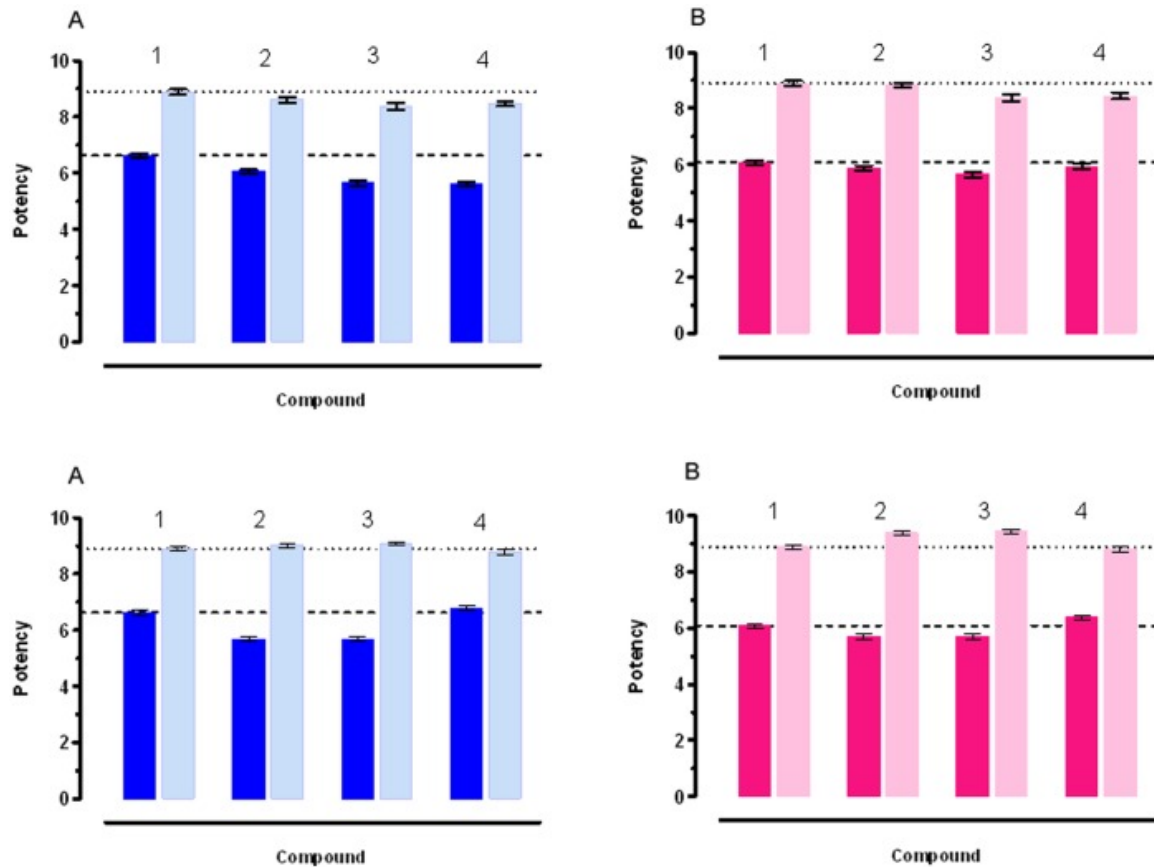


Figure 7

Similarly, the effect of Atropine was decreased: pA2 was reduced by 1.86 and 1.12 times respectively in the ileum and the colon. Both the effects were stronger in the ileum than in the colon: This finding is at variance with the histological damage, which is limited to the colon, resembling the histopathological features of UC. Seven days Curcuma extract administration improved the response to

Carbachol in the colon, but not in the ileum, both in comparison with the response of colon from mice with acute disease and mice assuming control diet, also if it did not completely restore the normal values. The response to Atropine was decreased both in the Curcuma added diet group and in the controls. In the ileum, Curcuma extract administration did not even partially restore the response to Carbachol and Atropine. In order to evaluate whether Curcuma extract had any effect on normal intestine and compare it, if any, with the effect of Curcuma on the intestine from mice with DSS induced acute colitis, we have administered Curcuma extract for 7 days to control mice. Curcuma extract inhibited the response to Carbachol in the ileum, by 1.69 and in the colon, by 1.20, while it increased in both the response to Atropine. The effect was greater in the ileum.

			Standard Dieta	CurcumaExt
ileum	CCh	pEC50	6.63±0.04	6.40±0.03
		<u>c</u>		<u>b</u>
	Atropine	pA2d	8.89±0.03	9.16±0.02
colon	CCh	pEC50	6.08±0.01	6.00±0.01
		<u>c</u>		
	Atropine	pA2d	8.89±0.01	9.47±0.02

Chronic colitis

Chronic colitis was induced in mice with DSS (2.5%w/v), three "8 days" cycles, with plain water between, for a total of 52 days, after which one group continued the control diet for 7 days, the other was switched to curcuma (200 mg/kg/day) over 7 days. After colitis induction, animals were either switched to curcuma or continued the usual diet. They were then sacrificed after 7, 14, 21 days and the two groups of animals were compared (Figure 8).

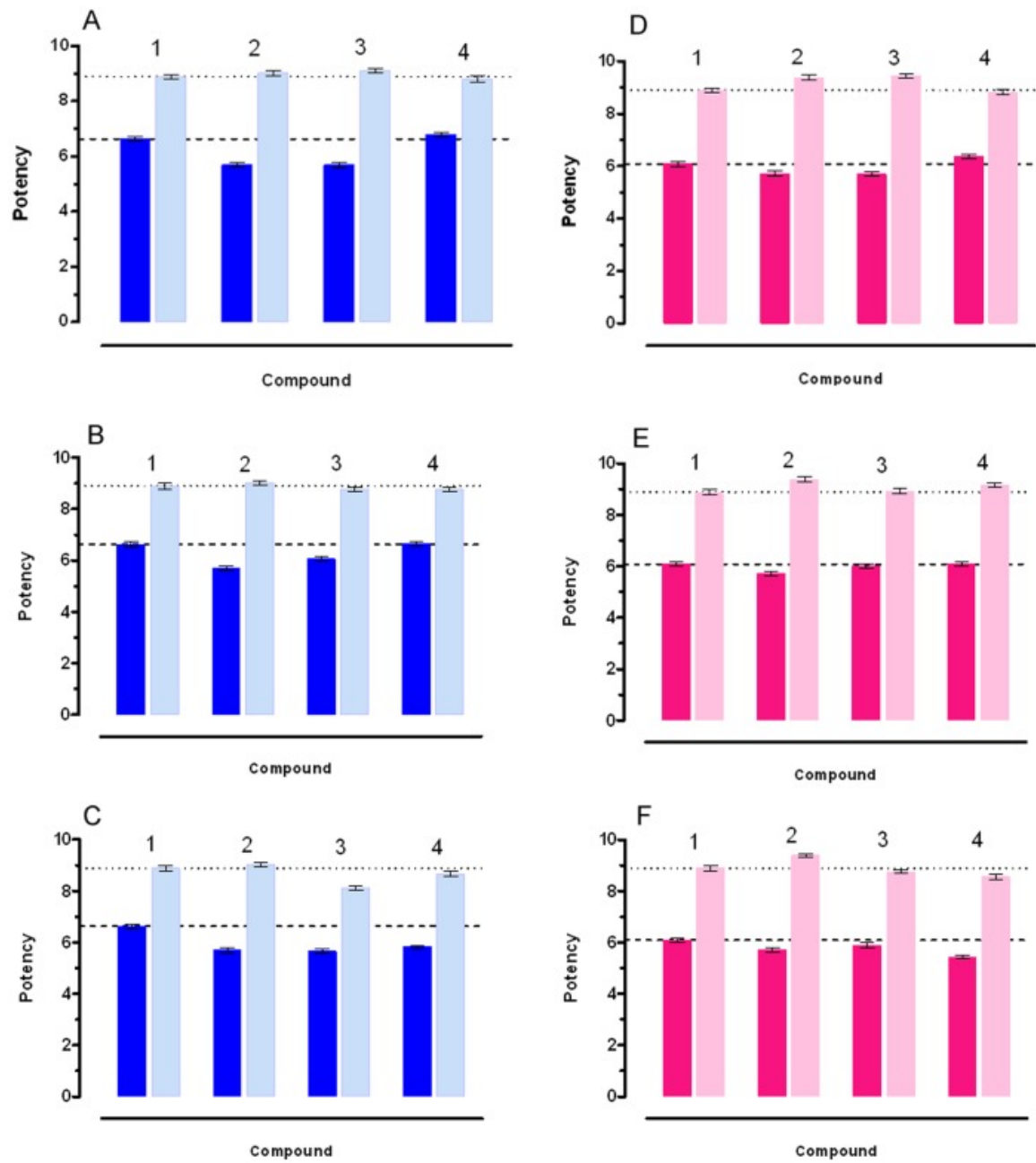


Figure 8

Discussion

There are few data available concerning the relationship between Curcuma and intestinal motility. In healthy humans, an indirect evidence that Curcuma activates bowel motility has been produced by hydrogen breath. On the contrary, Curcuma increases intestinal transit time in albino rats and ileal motility in Guinea Pig. The use of turmeric as an anti-inflammatory agent in IBD and the traditional empiric use of Curcuma as an antidiarrheal symptomatic drug in functional disorders of the gastrointestinal tract suggested an effect on intestinal motility. In IBD altered motility does not correspond to the location of inflammation and a reduced sympathetic regulation in uninflamed intestinal tracts has been demonstrated (39). The development of intestinal dysmotility may in turn result in abnormal growth of intestinal microflora, subsequently inducing a translocation of bacteria or bacterial products through the impaired mucosal barrier (40).

In humans, it is not clear whether IBD is associated with hyper or hypomotility (41). Reduced haustra formation, but augmentation colonic propulsive motility and diarrhea have been described (42,43). DSS colitis shares clinical and histopathological features of UC and reproduces a model of chemically driven colitis, where the damage of the epithelium is related to inflammation without an immune component. This model represents a good way to induce inflammation in the colon and to study its effect on motility. Spontaneous phasic contractions and Carbachol-evoked contractions of distal colon smooth muscles are reduced in DSS model of colitis (43,44). Conversely, increased Carbachol-evoked contractions and colonic smooth muscle hypercontractility were reported (45).

These findings may correlate with differences in experimental conditions, strain and gender differences in the susceptibility of DSS-colitis. In view of the possible gene differences, we have used male Balb/c mice: Balb/c mice are a strain commonly used for all-purpose laboratory investigations. Moreover males have been preferred over females to avoid the phasic influences of sexual hormones on gastrointestinal motility. In the present investigation, DSS induces deep disturbances in basal motor activity of ileum and colon: it is worthwhile noting that in acute colitis a hyperexcitability of the ileum is observed associated with a depressed motor activity in the colon, while a severe hyperexcitability is present both in ileum and in colon in the chronic colitis model. The abolition of any motor activity of the colon in acute experimental colitis is in agreement with the clinical condition of the toxic megacolon. We have chosen as reference of disturbed motility the ileal and colonic response to Carbachol and the inhibitory effect of Atropine on the Carbachol induced contraction. Carbachol and Atropine are respective agonist and antagonist at cholinergic muscarinic receptors. Both agonist and antagonist bind to the cholinergic receptors M(2) and M(3), present in mice small intestine and colon cellular membrane. In the present investigation, we have induced both chronic and acute colitis in mice, since the chronic model is more suitable for Curcuma treatment. The muscarinic receptor agonist Carbachol generated a smaller contractile force in the DSS-treated mice than in normal mice both in inflamed strip and uninflamed.

In this study we show that, in control conditions, Carbachol effect is more potent in the ileum than in the colon, while the antagonistic effect of Atropine is similar.

In vitro, Curcuma inhibits intestinal basal and Carbachol induced contraction in a non-competitive and reversible manner. The inhibition of basal intestinal motility demonstrates a direct effect on the intestinal muscular cells. The inhibition of Carbachol response is stronger in the ileum while the antagonistic effect of Atropine is increased in both. When orally administered to healthy animals, Curcuma has similarly shown a direct myorelaxant activity and an inhibition of Carbachol response on the ileum and colon, stronger on the former than on the latter. The effect of Atropine is conversely increased on both the intestinal tracts. These data represent the first attempt to characterize the myorelaxant effect of *Curcuma longa* on the ileum and colon. We have shown that this effect is independent of the anti-inflammatory effect. The mechanism of action is due both to a direct myorelaxant effect on the intestinal muscle layers and to a non-competitive and reversible inhibition of the cholinergic agent. The present study provides the rationale for the use of Curcuma Longa in motility disorders of IBD and suggests a possible application to functional motor disturbances of the gastrointestinal tract, due to the myorelaxant effect on the normal intestine, independent of the anti-inflammatory activity.

References

1. Strober W, Fuss I, Mannon P (2007) The fundamental basis of inflammatory bowel disease. *J Clin Invest* 117: 514–521.
2. Xavier RJ, Podolsky DK (2007) Unravelling the pathogenesis of inflammatory bowel disease. *Nature* 448: 427–34.
3. Triantafillidis JK, Merikas E, Georgopoulos F (2011) Current and emerging drugs for the treatment of inflammatory bowel disease. *Drug Des Devel Ther* 5: 185–210.
4. Ammon HP, Wahl MA (1991) Pharmacology of *Curcuma longa*. *Planta Med* 57: 1–7.
5. Singh AK, Sidhu GS, Deepa T, Maheshwari RK (1996) Curcumin inhibits the proliferation and cell cycle progression of human umbilical vein endothelial cell. *Cancer Lett* 107: 109–15. [[PubMed](#)]
6. Negi PS, Jayaprakasha GK, Jagan Mohan Rao L, Sakariah KK (1999) Antibacterial activity of turmeric oil: a byproduct from curcumin manufacture. *J Agric Food Chem* 47: 4297–4300.
7. Jain SK (1994) Ethnobotany and research on medicinal plants in India. *Ciba Found Symp* 185: 153–64.
8. Huang TS, Lee SC, Lin JK (1991) Suppression of c-Jun/AP-1 activation by an inhibitor of tumor promotion in mouse fibroblast cells. *Proc Natl Acad Sci USA* 88: 5292–5296.
9. Xu YX, Pindolia KR, Janakiraman N (1997) Curcumin, a compound with anti-inflammatory and anti-oxidant properties, down-regulates chemokine expression

in bone marrow stromal cells. *Exp Hematol* 25: 413–422.

10. Ahmed T, Gilani AH (2008) Inhibitory effect of curcuminoids on acetylcholinesterase activity and attenuation of scopolamine-induced amnesia may explain medicinal use of turmeric in Alzheimer's disease. *Pharmacol Biochem Behav* 91: 554–9.

11. Singh G, Kapoor IP, Singh P, de Heluani CS, de Lampasona MP, et al. (2010) Comparative study of chemical composition and antioxidant activity of fresh and dry rhizomes of turmeric (*Curcuma longa* Linn.). *Food Chem Toxicol*. 48: 1026–31.

12. Camacho-Barquero L, Villegas I, Sánchez-Calvo JM, Talero E, Sanches-Fidalgo S, et al. (2007) Curcumin, a *Curcuma longa* constituent, acts on MAPK p38 pathway modulating COX-2 and iNOS expression in chronic experimental colitis. *Int Immunopharmacol* 3: 333–42.

13. Claramunt RM, Bouissane L, Cabildo MP, Cornago MP, Elguero J, et al. (2009) Synthesis and biological evaluation of curcuminoid pyrazoles as new therapeutic agents in inflammatory bowel disease: effect on matrix metalloproteinases. *Bioorg Med Chem* 171: 290–6.

14. Bharti AC, Donato N, Singh S, Aggarwal BB (2003) Curcumin (diferuloylmethane) down-regulates the constitutive activation of nuclear factor-kappa B and I-kappaB kinase in human multiple myeloma cells, leading to suppression of proliferation and induction of apoptosis. *Blood* 101: 1053–62.

15. Han SS, Keum YS, Seo HJ, Surh YJ (2002) Curcumin suppresses activation of NF-kappaB and AP-1 induced by phorbol ester in cultured human

promyelocytic leukemia cells. *J Biochem Mol Biol* 35: 337–42.

16. Singh S, Aggarwal BB (1995) Activation of transcription factor NF-kappa B is suppressed by curcumin (diferuloylmethane)[corrected]. *J Biol Chem* 270: 24995–25000.

17. Xu YX, Pindolia KR, Janakiraman N, Chapman RA, Gautam SC (1977) Curcumin inhibits IL1 alpha and TNF-alpha induction of AP-1 and NF-kB DNA-binding activity in bone marrow stromal cells. *Hematopathol Mol Hematol* 11: 49–62.

18. Deguchi Y, Andoh A, Inatomi O, Yagi I, Bamaba S, et al. (2007) Curcumin prevents the development of Dextran Sulfate Sodium (DSS)-induced experimental colitis. *Dig Dis Sci* 52: 2993–8.

19. Kim GY, Kim KH, Lee SH, Yoon MS, Lee HJ, et al. (2005) Curcumin inhibits immunostimulatory function of dendritic cells: MAPKs and translocation of NF-kappa B as potential targets. *J Immunol* 174: 8116–24.

20. Shimouchi A, Nose K, Takaoka M, Hayashi H, Kondo T (2009) Effect of dietary turmeric on breath hydrogen. *Dig Dis Sci* 54: 1725–9.

21. Sugimoto K, Hanai H, Tozawa K, Aoshi T, Uchijima M, et al. (2002) Curcumin prevents and ameliorates trinitrobenzenesulfonic acid-induced colitis in mice. *Gastroenterology* 123: 1912–22.

22. Ukil A, Maity S, Karmakar S, Datta N, Vedasiromoni JR, et al. (2003) Curcumin, the major component of food flavorturmeric, reduces mucosal injury in trinitrobenzenesulphonic acid induced colitis. *Br J Pharmacol* 139: 209–18

23. Salh B, Assi K, Templeman V, Parhar K, Owen D, et al. (2003) Curcumin

attenuates DNB-induced murine colitis. *Am J Physiol, Gastrointest Liver Physiol* 285: G235–43.

24. Hanai H, Iida T, Takeuchi K, Watanabe F, Maruyama Y, et al. (2006) Curcumin maintenance therapy for ulcerative colitis: randomized, multicenter, double-blind, placebo-controlled trial. *Clin Gastroenterol Hepatol* 12: 1502–6.

25. Jian YT, Mai GF, Wang JD, Zhang YL, Luo RC, Fang YX (2005) Preventive and therapeutic effects of NF-kappaB inhibitor curcumin in rats colitis induced by trinitrobenzene sulfonic acid. *World J Gastroenterol* 11: 1747–52.

26. Jacobson K, McHugh K, Collins SM (1995) Experimental colitis alters myenteric nerve function at inflamed and non-inflamed sites in the rat. *Gastroenterology* 109: 718–22.

27. Aube AC, Cherbut C, Barbier M, Xing JH, Roze C, et al. (1999) Altered myoelectrical activity in non-inflamed ileum of rats with colitis induced by trinitrobenzenesulphonic acid. *Neurogastroenterol Motil* 11: 55–62.

26. Blandizzi C, Fornai M, Colucci R, Antonioli L, Bernardini N, et al. (2003) Altered prejunctional modulation of intestinal cholinergic and noradrenergic pathways by alpha2-adrenoceptors in the presence of experimental colitis. *Br J Pharmacol* 139: 309–20.

29. Kohno N, Nomura M, Okamoto H, Kaji M, Ito S (2006) The use of electrogastrography and external ultrasonography to evaluate gastric motility in Crohn's disease. *J Med Invest* 53(3–4): 277–84.

30. Tomita R, Munakata K, Tanjoh K (1998) Role of non-adrenergic non-cholinergic inhibitory nerves in the colon of patients with ulcerative colitis. *J*

Gastroenterol 33: 48–52.

31. Vasina V, Barbara G, Talamonti L, Stanghellini V, Tonini M, et al. (2006) Enteric neuroplasticity evoked by inflammation. *Auton Neurosci* 126–127: 264–72.

32. Qureshi S, Song J, Lee HT, Koh SD, Hennig GW, Perrino BA (2010) CaM kinase II in colonic smooth muscle contributes to dysmotility in murine DSS-colitis. *Neurogastroenterol Motil* 22: 186–186–95, e64.

33. Motagally MA, Neshat S, Lomax AE (2009) Inhibition of sympathetic N-type voltage-gated Ca²⁺ current underlies the reduction in norepinephrine release during colitis. *Am J Physiol Gastrointest Liver Physiol* 296: G1077–84.

34. Sato K, Ninomiya H, Ohkura S, Ozaki H, Nasu T (2006) Impairment of PAR-2-mediated relaxation system in colonic smooth muscle after intestinal inflammation. *Br J Pharmacol* 148: 200–7.

35. Mizuta Y, Isomoto H, Takahashi T (2000) Impaired nitrergic innervation in rat colitis induced by dextran sulfate sodium. *Gastroenterology* 118: 714–23.

36. Kumar A, Purwar B, Shrivastava A, Pandey S (2010) Effects of curcumin on the intestinal motility of albino rats. *Indian J Physiol Pharmacol* 54: 284–8.

37. Itthipanichpong C, Ruangrunsi N, Kemsri W, Sawasdipanich A (2006) Antispasmodic effects of curcuminoids on isolated guinea-pig ileum and rat uterus. *J Med Assoc Thai* 86 Suppl 2S2999–309.

38. Wirtz S, Neufert C, Weigmann B, Neurath MF (2007) Chemically induced mouse models of intestinal inflammation. *Nat Protoc* 2: 541–6.

39. Linden DR, Sharkey KA, Ho W, Mawe GM (2004) Cyclooxygenase-2

contributes to dysmotility and enhanced excitability of myenteric AH neurones in the inflamed guinea pig distal colon. *J Physiol* 557: 191–205.

40. Lomax AE, Fernandez E, Sharkey KA (2005) Plasticity of the enteric nervous system during intestinal inflammation. *Neurogastroenterol Motil* 17: 4–15.

41. Akiho H, Ihara E, Motomura Y, Nakamura K (2011) Cytokine-induced alterations of gastrointestinal motility in gastrointestinal disorders. *World J Gastrointest Pathophysiol* 15 2(5): 72–81.

42. Reddy SN, Bazzocchi G, Chan S, Akashi K, Villanueva-Meyer J, et al. (1991) Colonic motility and transit in health and ulcerative colitis. *Gastroenterology* 101: 1289–97.

43. Kinoshita K, Sato K, Hori M, Ozaki H, Karaki H (2003) Decrease in activity of smooth muscle L-type Ca²⁺ channels and its reversal by NF-kappaB inhibitors in Crohn's colitis model. *Am J Physiol - Gastrointestinal and Liver Physiology* 285: G483–G493.

44. Myers BS, Martin JS, Dempsey DT, Parkman HP, Thomas RM, et al. (1997) Acute experimental colitis decreases colonic circular smooth muscle contractility in rats. *Am J Physiol - Gastrointestinal and Liver Physiology* 273: G928–G936.

45. Kondo T, Nakajima M, Teraoka H, Unno T, Komori S, et al. (2011) Muscarinic receptor subtypes involved in regulation of colonic motility in mice: functional studies using muscarinic receptor-deficient mice. *Eur J Pharmacol* 670: 236–43.

2. Characterization of the role of CEACAM5 in the intestinal immunoregulation

2.1 BACKGROUND

The intestinal epithelial barrier is a dynamic structure that separates the intestinal luminal content (antigens from the diet and microbioma) from the underlying immune system in the lamina propria. It is a mechanic barrier itself because regulate the antigens trafficking by its nature and composition and because it regulates the crosstalk with the cell of the immune system. Epithelial cells are placed at the center of this structure. On the luminal side they regulate nutrient absorption as well as mucous layer composition; on the basolateral side they talk with the immune cells.

Mayer's lab among others has well demonstrated the role of intestinal epithelia cells as non-professional antigen presenting cells (Figure1).

The nature of the immune response in the intestine is one of immunosuppression or controlled inflammation. The suppressive state is dictated by several factors including regulatory T cells, non-T cells and unique antigen presenting cells. It is well known that failure to control immune responses may lead to inflammatory bowel disease (IBD) such as Crohn's disease (CD) and ulcerative colitis (UC). In the normal colon, it has been suggested that the immunosuppressed state may be related to unique population of antigen presenting cells and unique populations of T cells.

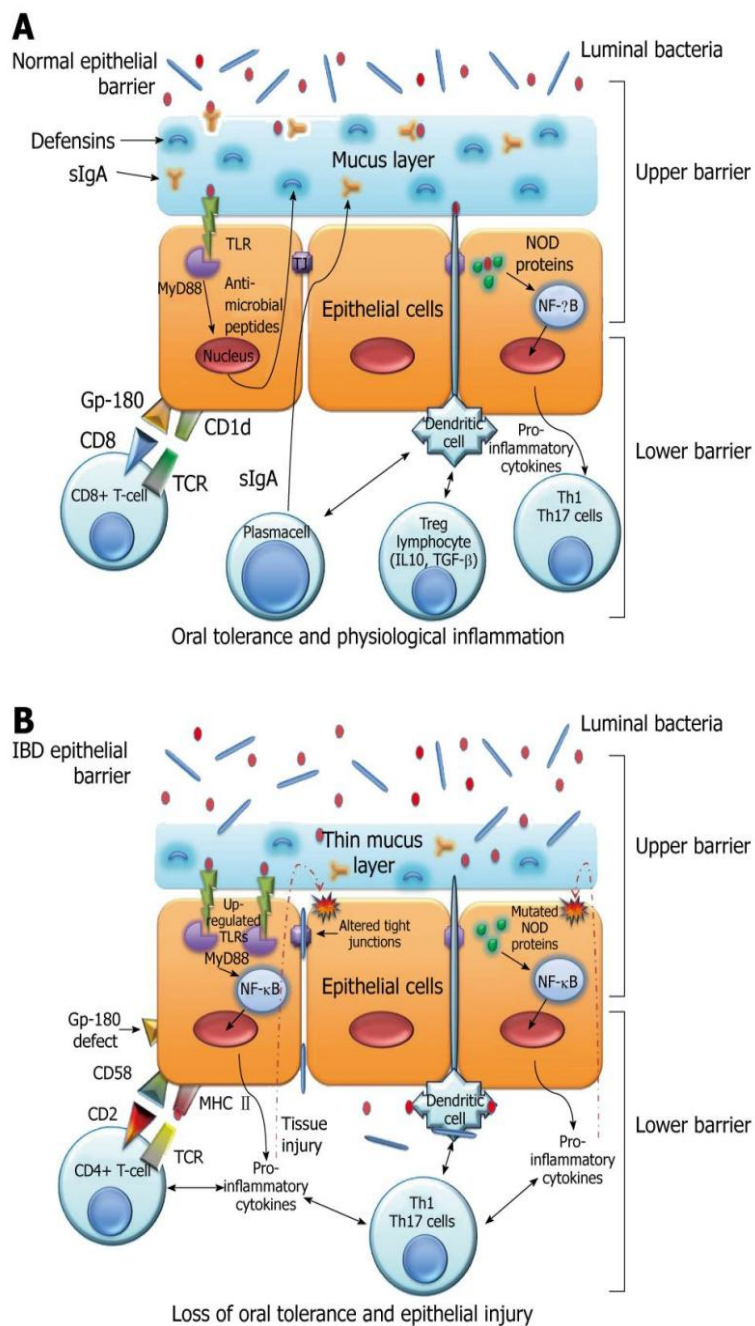


Figure 1: The epithelial barrier system. A: Normal epithelial barrier; B: Inflammatory bowel disease (IBD) epithelial barrier. TLR: Toll-like receptors; MyD88: myeloid differentiation factor 88; TJ: Tight junctions. **World J. Gastroenterol. 2010 September 14; 16(34): 4264–4271**

Our lab has proposed that IECs can act as nonprofessional antigen presenting cells. We have described that IECs interact with T cells through a unique complex, formed by a carcinoembryonic antigen-related cell adhesion molecule (CEACAM) subfamily member (gp180) and the nonclassical class I molecule CD1d resulting in the expansion of CD8⁺ T regs. (1-7). We characterized gp180 as a surface glycoprotein recognized by two anti-epithelial cell mAbs, B9 and L12. We demonstrated that gp180 (mAb B9 affinity purified material) binds to CD8, activates CD8 associated kinase p56Lck and binds to CD1d. The two mAbs (B9 and L12) block the selective proliferation of CD8⁺ T cells and inhibit the phosphorylation of the CD8 associated kinase p56Lck in IEC: T cell co-cultures (8-17). Furthermore, we documented decreased expression of gp180 in non-inflamed IBD tissues with mAb B9. This defect correlated with the inability of IBD IECs to activate CD8⁺ Treg cells (18).

CEA (CEACAM5) was first described in 1965 by Gold and Freedman as a tumor associated antigen in human colon cancer tissue extracts. It was hypothesized that CEA was an oncofetal antigen – expressed during fetal life, absent in healthy adult and re-expressed when epithelial cells became malignant. Nowadays, it is well established that CEA is expressed in adult tissue as well. The CEA gene family belongs to the immunoglobulin gene superfamily. Two subgroups exist: CEA and the pregnancy specific glycoprotein (PSG) subgroups. CEA subfamily proteins are cell surface proteins whereas the PSG are secreted proteins. CEA subfamily proteins are heavily glycosylated and can be either transmembrane or GPI-linked. Analysis of the amino acid sequence reveals distinct domain

organization amongst the family. Two types of immunoglobulin (Ig) domains are seen: an N-terminal domain of 108 amino acids homologous to the Ig variable domain (IgV-like) and between zero and six domains homologous to the Ig constant domain to the C2 set (IgC-like). The IgC domain may be either of type A containing 92 amino acids or type B containing 85 amino acids. According to this designation the domain formula is N-A1-B1-A2-B2-A3-B3. CEA is expressed in columnar intestinal epithelial cells and goblet cells in the colon, in mucous neck cells and pyloric mucous cells in the stomach, in squamous epithelial cells from the tongue, esophagus and cervix, in secretory epithelia, and ducts cells of sweat glands and in epithelial cells from the prostate. CEA has been described to play a role in cell-cell adhesion through homotypic and heterotypic anti-parallel N-domain to N-domain interactions or N-domain to membrane proximal domain (two points of interaction between two neighboring cells). Moreover, CEA functions as signal transduction through the modified ITAM (immunoreceptor tyrosine-based activation domain)/ITIM (immunoreceptor tyrosine-based inhibition motif) in a long cytoplasmic tail isoform of transmembrane CEA subfamily proteins. Various reports have described a role for CEA family members in cell-cell adhesion engaging homotypic and heterotypic interactions through their N-terminal domains. Several members have been described to act as pathogen sensors suggesting a possible role of CEA in host-pathogen crosstalk. (19-29).

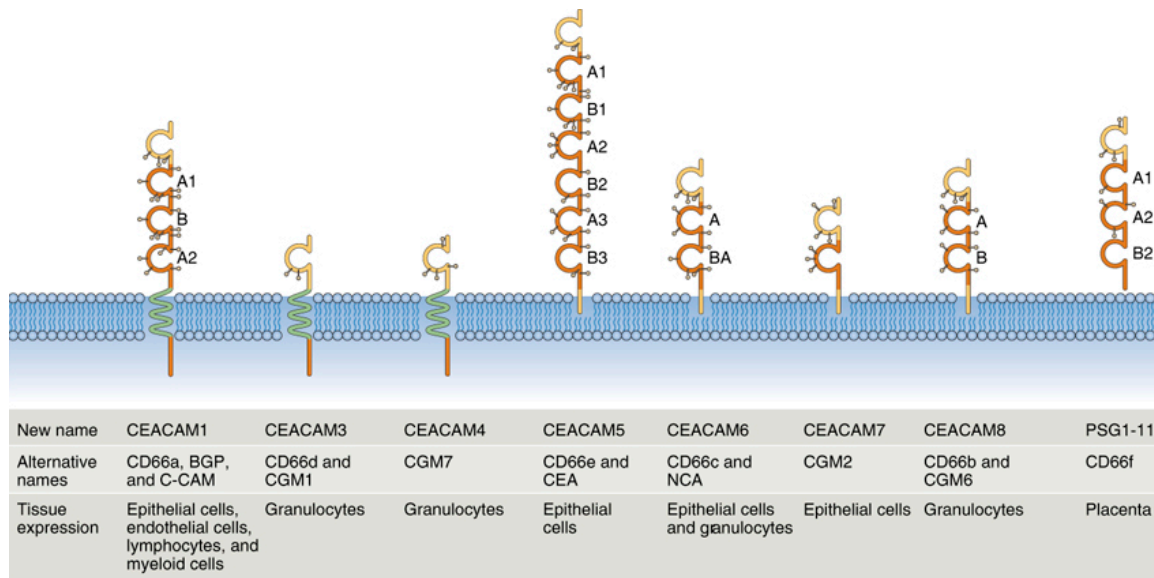


Figure 2: CEACAM family members. *Mucosal Immunology* (2008) **1** (Suppl 1), S39–S42. doi:10.1038/mi.2008.50

Our hypothesis guiding this proposal is that gp180 is CEACAM5, one of the member of the CEACAMs family and that an unique set of interactions between CEACAM5 and CD1d form a complex that binds to CD8 and the TcR and results in the activation of CD8 Tregs. In fact, defining the nature of the intermolecular interactions between CEACAM5, CD1d and CD8 will help to identify the mechanism of activation of TrE cells and to develop mechanisms to promote this interaction in Crohn’s disease, where we have shown a defect in the activation of CD8+ Treg cells (related to a defect in the expression of CEACAM5). Furthermore, as a result of these studies, we can enhance mucosal immunity (as in CEACAM5 expressing tumors) by blocking the interaction of CEACAM5 with

CD8 with interfering small peptides. Understanding the role of CEACAM5 in the mucosal immune system in normals will allow us to define the nature of the defects in expression of these molecules in IBD and potentially develop approaches to overcome the defects seen. We will initiate these studies by determining how CEACAM5 is involved in the activation of CD8+ regulatory T cells and assessing whether the B9 binding site on CEACAM5 overlaps with the CD8 binding site.

2.2 SPECIFIC RESEARCH OBJECTIVES

Specific Aim 1. Assess whether gp180 is homologous to CEACAM5.

Specific Aim 2. Define CEACAM5/CD1d interactions.

Specific Aim 3. Define CEACAM5/CD8 α interaction and CEACAM5 functionality.

Specific Aim 4. Assess whether mutation in the N domain of CEACAM5 affect CEACAM5/CD8 α interaction

Specific Aim 5. Design small (CEACAM5) peptides from the N domain and assess their ability to activate CD8-associated Lck kinase.

2.3 METHODS OF APPROACH

Purification and sequencing of gp180

gp180 purification from human intestinal epithelial cells (IECs) was performed using a mAb B9 affinity column as described previously (8). Protein sequencing was accomplished by the Protein DNA Core at the Rockefeller University.

Construction of vectors

Dual expression vector of CEACAMs and CD1d: cDNAs for CEACAM1, CEACAM5, CEACAM6 and CD1d (Genbank accession no NM_001024912, NM_004363, NM_002483 and NM_001766) were obtained by RT-PCR from human IEC mRNA. All of the primers are shown in Table 1.

	Forward	Reverse
CEACAM1	5'-CCGCTAGCATGGGGCACCTCTC-3'	5'-CCCTCGAGTTACTGCTTTTTTAC-3'
CEACAM5	5'-CCGCTAGCATGGAGTCTCCCTC-3'	5'-CCCTCGAGCTATATCAGAGCAAC-3'
CEACAM6	5'-CCCTCGAGCTATATCAGAGCAAC-3'	5'-CCCTCGAGCTATATCAGAGCCAC-3'
CD1d	5'-CCGGATCCACCATGGGGTGCCTGCTG-3'	5'-CCCTTAAGTCACAGGACGCCCTG-3'

Table 1: CEACAMs and CD1d primers sequences

An internal ribosomal entry site (IRES) was amplified from the pIRES-EGFP plasmid (Clontech) using forward (5'-CCGAATTCATTCCGCCCTCTCC-3') and reverse (5'-CCGGATCCGGGTTGTGGCAAGC) primers. Then the IRES alone (IRES), IRES-CD1d (CD1d), IRES-CEACAM5-GFP as well as IRES-CD1d simultaneously with CEACAM1, CEACAM5 or CEAMCAM6 (CEACAM1.CD1d, CEACAM5.CD1d and CEACAM6.CD1d) were subcloned into pcDNA3.1(-) vector (Invitrogen).

Vectors expressing mutants of CEACAM5: Wild-type (WT) CEACAM5 construct was used as a template for PCR-generated mutant constructs. For sequential C-terminal truncation, the forward primer for WT was used and the reverse primers for all the deletion mutants including B3, A3B3, B2A3B3, B3.1, B3.2, B3.3, B3.4, B3.5 are shown in Table 2.

	Reverse
ΔB3	5'-GCGGCCGCCTACGGCCCATAGAGGACATCCAGG-3'
ΔA3B3	5'-GCGGCCGCCTAGGGCAGCTCCGCAGAGACTGTGAT-3'
ΔB2A3B3	5'-ATAGCGGCCGCCTATGGGCCATAGAGGACATT-3'
ΔB3.1	5'-ATAGCGGCCGCCTAGCCAGTAGCCAAGTTAGA-3'
ΔB3.2	5'-ATAGCGGCCGCCTAATTATTTGGCGTGATTTT-3'
ΔB3.3	5'-ATAGCGGCCGCCTATTGCTGCGGTATCCCATT-3'
ΔB3.4	5'-ATAGCGGCCGCCTATGGGTTAGAGGCCGAGT-3'
ΔB3.5	5'-ATAGCGGCCGCCTAGTAAGACGAGTCTGGG-3'

Table 2: ΔB3, ΔA3B3, ΔB2A3B3, ΔB3.1, ΔB3.2, ΔB3.3, ΔB3.4, ΔB3.5 primers sequences

Overlap extension PCR was performed to construct the expression vector for deletion of the A2-domain. The forward primer for the WT CEACAM5 and reverse primer (5'-GACGACCCCACCATTTCCTCA-3') were used to generate fragment 1. The forward primer (5'-GGTGGGGTCGTCGGGTGGCTCTGCATA-3') and reverse primer for WT CEACAM5 were used to generate fragment 2. Then the cDNA with the deletion of A2-domain was generated from fragment 1 and 2 using primers for WT. The PCR fragments were subcloned into CD1d-pcDNA3.1(-). The p91023(B) vectors encoding WT and mutant CEACAM5 with deletion of N42 to I46 residues in the N-terminal domain (N⁴²RQII), point mutations in the N-terminal domain (K35A and N70,81A) and CEACAM8 were generated. The sequences of all constructs were confirmed by DNA sequencing. CD8α cDNA was provided by Dr P.

Kavathas (Yale School of Medicine) and the extracellular domain was sub-cloned into a pcDNA 3.1/V5-His vector.

Cell culture and transfection

For transfection, a human embryonic kidney (293T), an ovarian Chinese hamster carcinoma (CHO) and a melanoma (FO-1) cell lines were used. The cells were grown at 37⁰C in Dulbecco's modified Eagle's medium (GIBCO, Carlsbad, CA) or in F-12K medium (ATCC) containing 10% fetal bovine serum (FBS), in a humidified 5% CO₂ incubator. Cells were transfected in 6-well plates using Lipofectamine-2000 (Invitrogen) with 4 µg of pcDNA3.1 vectors encoding CD1d alone or along with wild-type or truncated CEACAM5. Untransfected or cells transfected with IRES were used as controls. For the generation of stable cells expressing wild-type and mutant CEACAM5, cells were transfected in 100 mm culture plates with 12 µg of p91023(B) expression vectors encoding wild-type or mutant CEACAM5 together with 12 µg of pcDNA3.1. The stable cells were established after selection with 3 mg/ml Geneticin (G418, Sigma). Stable cells were treated with 0.1unit/ml phospholipase C, phosphatidylinositol specific enzyme (PIPLC, Sigma) for 1 h at 37⁰C. The supernatant was collected and subjected to Western blotting using mouse Col-1 and mouse anti-gp180 (B9) monoclonal antibodies. Human IEC cell lines, HT29 and T84, were used as positive controls.

Western Blots

The protein samples were subjected to 10% SDS-PAGE gels, transferred to nitrocellulose membranes and blocked with 5% milk for 1 h at room temperature.

Membranes were incubated with primary antibodies overnight at 4°C, washed with (phosphate buffered saline) PBS containing 0.05% Tween-20, and incubated with HRP-conjugated secondary antibody (Cell Signaling) for 1 h at room temperature. The proteins were visualized using a chemiluminescent HRP substrate (Millipore).

Flow cytometry

Trypsinized transfected CHO cells (1×10^6) expressing CEACAM5, 1, 6 and 8 were incubated with the appropriate mAbs B9 and B18 diluted in 100 μ L PBS containing 0.2% FBS and followed by a second incubation on ice with FITC-labeled F(ab)₂ fragments of immunosorbent-purified goat anti-mouse IgG.

3G8 cells were treated for different time points (2, 8, 10, 15 min) at 37°C with anti-CD8 mAb (OKT8) at 5 μ g/ μ L, H₂O₂ at 10 mM, CEACAM5 supernatant (Sup1) from PIPLC-293T cells expressing CEACAM5 and purified CEACAM5 peptide at 20 μ g/mL. Stimulation was stopped by fixing with 4% formaldehyde for 10 min at room temperature. Subsequently, cells were permeabilized with ice-cold methanol for 20 min, washed with PBS containing 0.2% FBS and stained with anti-phospho-Lck Ab (BD Biosciences). The cells were then re-suspended in PBS plus 0.2% FBS, data acquired using the FACScan system and data analyzed with FlowJo analysis software.

Co-immunoprecipitation

293T cells were used for co-immunoprecipitation 48h after transfection with the corresponding vectors as described above. Cell extracts (150 μ g of protein) were incubated with either 2 μ g of mouse IgG2b anti-CD1d (D5), mouse IgG1 anti-

gp180 (B9), isotype control mouse IgG2b or mouse IgG1 for 4h at 4°C, followed by the addition of 10 µl protein G Sepharose (Amersham Biosciences) for 12h. Pellets were washed three times with RIPA buffer (10 mM Tris, pH 8.0, 1.0 mM EDTA, 0.5% Nonidet P-40, 0.1 M NaCl), boiled in SDS sample buffer, and resolved on SDS-PAGE gels. After transferring to nitrocellulose, an anti-CEA mAb (Col-1) (Dako) followed by a CD1d mAb D5 Western blot was performed.

Absorption assay

10 µL of PIPLC treated supernatants from 293T/CEACAM5 cells or from confluent T84 cells were incubated on ice with 14×10^6 3G4 (mouse T cell hybridoma transfected with human CD4 cDNA) or 3G8 (mouse T cell hybridoma transfected with human CD8 cDNA) cells for 1 hour. After incubation, 20 µL of RPMI were added to each tube to facilitate collection of the absorbed supernatants. Supernatants (Sup2) were collected following centrifugation at 13,000 rpm for 2 minutes. The entire 30 µL was resolved in 8% SDS-PAGE and subjected to Western Blot analysis. 5×10^6 3G4 cells or 3G8 cells re-suspended in 50 µL of serum free RPMI medium were incubated on ice for 30 minutes, then co-incubated for 2, 8 or 15 minutes at 37°C with 293T/CEACAM5 or 293T/vector-PIPLC (equivalent of 2×10^6 cells) bound to protein G-sepharose 4B beads via anti-CEA mAb Col-1 and rabbit anti-mouse IgG (RAM) (10µL beads medium). 3G4 or 3G8 cells kept on ice were used as controls. At the end of each time point, samples were placed on ice; ice-chilled stop buffer added and samples were centrifuged at 13,000 rpm for 1 minute at 4°C. Supernatants were completely removed; cell pellets were immediately lysed in SDS-PAGE sample

loading buffer and samples were subsequently subjected to Western Blot analysis using a horseradish peroxidase conjugated-4G10 (anti-phospho-tyrosine mAb) as the probing antibody. The same membrane was re-probed for Ick and beta-actin, as internal loading controls.

Protein purification

The supernatant obtained from treated PIPLC transfected CHO cell lines was collected and subjected to mouse anti-CEA (Col-1) mAb Western blot. Supernatants expressing CEA were subjected to a Col-1 Ab (A/B domain specific) purification column, to dialysis using dialysis membrane tubing with MWCO of 12000-14000 and to concentration using Vivaspin 6 columns. Supernatant obtained from CD8 α transfected 293T cells containing the extracellular domain of CD8 α was collected and subjected to a mouse monoclonal anti-CD8 α Antibody Western Blot. Supernatant expressing CD8 α was purified using the Probond purification System-Invitrogen specific for polyhistidine-containing recombinant proteins. Eluted protein was then subjected to dialysis and concentration. Eluted proteins were finally subjected to mAb Col-1 (Zymed) and mAb CD8 α Western Blot (Santa Cruz) to confirm the presence of full length and mutants CEACAM5s and CD8 α .

Biacore Kinetic Analyses

As assay buffer, we used 10 mM HEPES buffer (pH 7.4), 150 mM NaCl, 3mM EDTA, 0.005% P20 (polyoxyethylenesorbitan); as regeneration buffer we used 50mM Tris, 2M NaCl, pH 7.3 and as conjugation buffer we used 10 mM sodium acetate buffer (pH 5.0). Purified CD8 α protein was directly immobilized to the

high capacity carboxymethylated dextran and covalently attached to a gold surface (CM5 chip) by amine coupling chemistry. The amount (R_L) of protein to be captured on the chip was determined by the following formula: $R_{Max} = MW_A / MW_L \cdot R_L$ where MW_A is the molecular weight of the analyte (CEACAM5) (180 KDa) and MW_L is the molecular weight of the ligand (CD8 α) (19 KDa). R_{Max} corresponds to the maximum resonance unit that we obtained during analyses. We set R_{Max} below 50 for antibody/antigen interactions. R_L corresponds to the refractory index of the ligand and is expressed in resonance units (RU). R_{MAX} of 50 was $R_L = 50 \times 19 / 180 = 5.3$. We captured the ligand onto the chip until it reached 5.3 RU. RU is a Resonance Unit generated by the shift of refractory index due to ligand-analyte interactions on a sensor chip. KD is defined as $KD = K_d/K_a$.

Biacore measures real time K_a (on rate) and K_d (off rate) based on its curve fitting program. The flow rate used for capturing ligand is 5 ml/min. For kinetic analysis, the flow rate of 30 ml/min is used for the analyte. The first run is the scouting analysis using high concentrations of analyte. For the assays we used 200 nM. At this concentration, binding should be observed even if the ligand binding affinity is weak. The scouting analysis provides a rough K_D . Based on the rough K_D value, full kinetics analyses are performed using 5 analyte concentrations slightly above the K_D to zero. Chi square (χ^2) analysis on the K_D values obtained from each analyte concentration was performed to determine the statistical accuracy of the measured K_D . χ^2 value of ~ 2 is considered significant (accurate) and below 1 is highly significant (highly accurate). After each assay,

the chip is treated with 50mM Tris, 2M NaCl, pH 7.3 to remove the ligand and the analyte for regeneration.

2.4 RESULTS

Purified gp180 bears sequence homology to CEA

gp180, purified by immunoaffinity using mAb B9, was subjected to amino terminal sequencing by Edman degradation. Over the first 25 amino acids, there was 100% sequence homology with CEACAM5. The sequences of other CEACAM family members were similar but show clear differences with the sequence obtained. The congruence between the molecular weights and the N-terminal amino acid sequences between gp180 and CEACAM5 strongly supports the contention that gp180 and CEACAM5 are identical.

gp180	LTIESTPFNVAEGK-- LLLVHNLQPQLF
	LTIESTPFNVAEGK LLLVHNLQP LF
CEACAM5	LTIESTPFNVAEGKEVLLLHNLQPQLF

CEACAM5 transfectants express the B9 epitope

Given the amino acid sequence homology to CEACAM5, we determined whether this member of the CEA family expressed the epitope recognized by mAb B9. A CEACAM5-GFP bicistronic construct was transfected into 293T cells and FO-1 cells. GFP expressing 293T cells co-expressed a molecule recognized by mAb B9 (Figure 3). In addition, CHO cells transfected with CEACAM5 were shown by

FACS analysis to bind mAb B9 (Figure 4). These data suggest that CEACAM5 contains the B9 epitope.

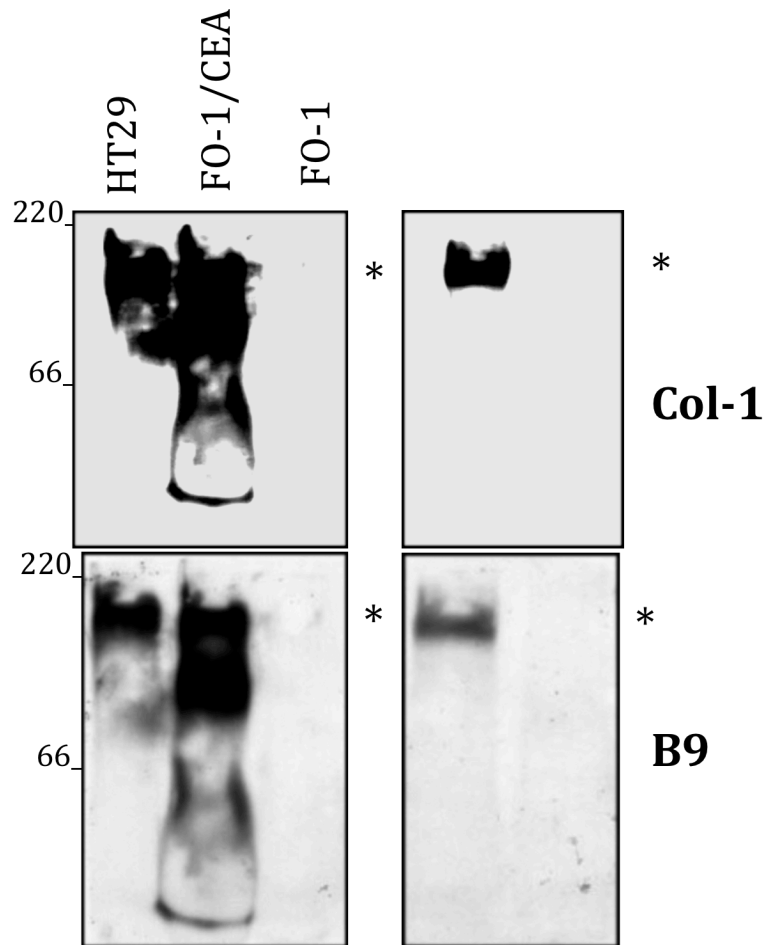


Figure 3: CEACAM5 is recognized by B9 mAb

Immunoblotting for CEACAM5 in lysates obtained from HT29, as well as FO-1 and 293T cells transfected with CEACAM5. B9 and Col-1 monoclonal antibodies were used for Western blotting. Non-transfected FO-1 and 293T cells were used as negative control. Data are representative of three independent experiments.

mAb B9 recognizes other CEACAM family members

CHO cells transfected with CEACAM6, CEACAM1-4L (a splice variant of BGP) and CEACAM8 were stained with two mAbs B9 and B18 and analyzed by flow cytometry. In addition to CEACAM5, mAb B9 recognized CEACAM6, CEACAM1-4L, and CEACAM8 transfectants but not a non-transfected CHO cell line (Figure 4). Thus several CEACAM family members share the B9 epitope in their N-domains and could conceivably share the immunosuppressive function of CEA.

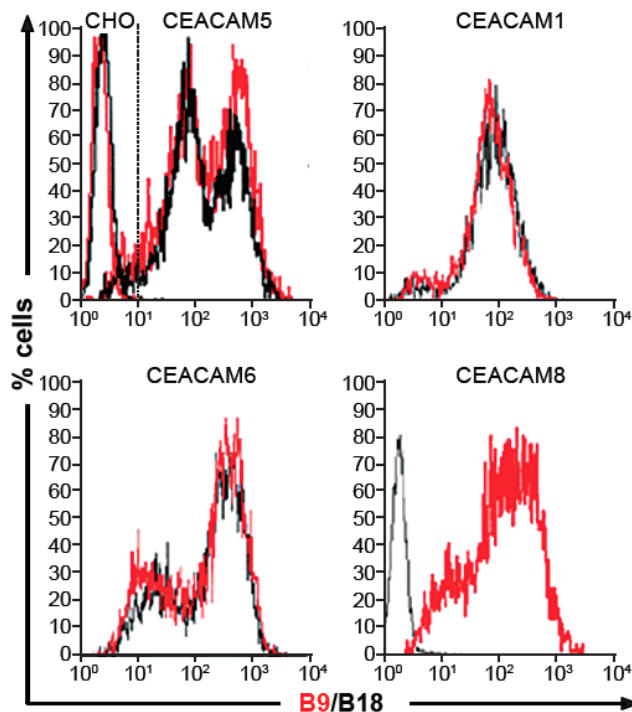


Figure 4: B9 recognizes different CEACAMs expressed on IECs

Cyto-fluorimetric profiles of CHO cells expressing CEACAM5 or CEACAM1-4L, CEACAM6 and CEACAM8, labeled with B9 or B18 mAbs. B9 can recognize all

four CEACAM members. Data are representative of three independent experiments.

CEACAM5 binds to CD1d through the B3 domain

To assess whether CEACAM5 binds CD1d as well as gp180 and which member of the CEACAM family has binding properties to CD1d, we co-expressed different CEACAMs and CD1d in 293T cells. The lysates were subjected to co-immunoprecipitation experiments using the anti-CD1d antibody D5. We show for the first time that CEACAM5 is the only CEACAM member expressed on IECs which interacts with CD1d (Figure 5).

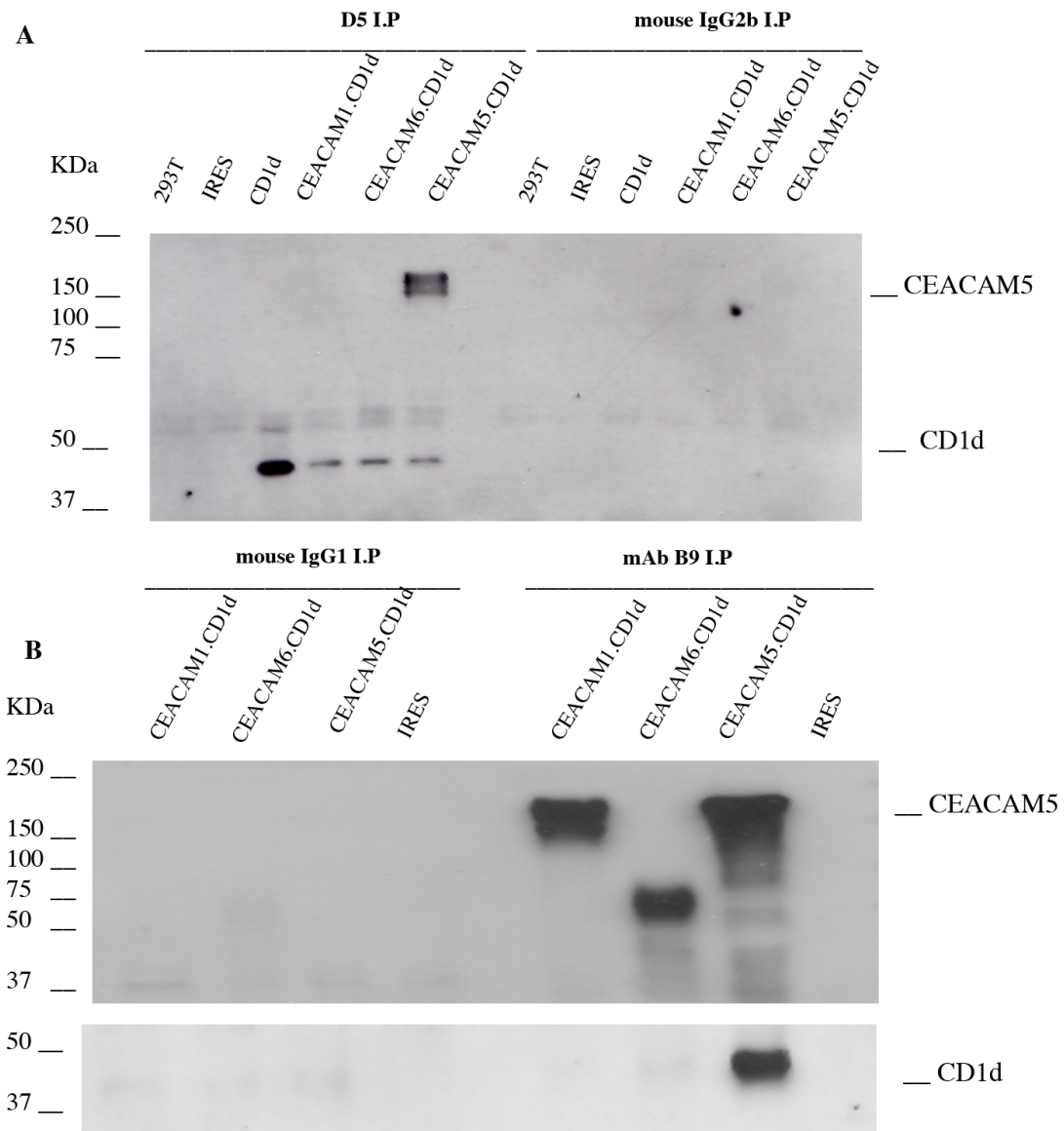


Figure 5. CEACAM5, but not CEACAM1 or CEACAM6 binds to CD1d.

293T cells were co-transfected with pcDNA3.1-IRES-CD1d alone or together with CEACAM1, CEACAM5 or CEACAM6. The cell lysate was co-immunoprecipitated with mouse IgG2b anti-CD1d (D5), or with mouse IgG1 anti-gp180 (B9) antibodies. Western blots were performed with Col-1 and D5 mAbs. Data are representative of three independent experiments.

All CEACAM family members contain an extracellular N-terminal IgV-like and various C-terminal IgC-like domains that are designated as type A or B domains. We compared the sequences of CEACAM1, 5, and 6 and limited homology in the A2 and B3 (B1 for CEACAM1 and CEACAM6) domains was found. We generated different deletion mutants of CEACAM5. Neither deletion of the N-terminal region nor of the A2 domain contributes to the interaction between CEACAM5 and CD1d (Figure 6). In contrast, sequential C-terminal truncations of each domain allowed us to determine that deletion of the B3-domain obliterated the ability of CEACAM5 to bind to CD1d (Figure 6). We then performed sequential deletions within the B3 domain and we found that the interaction between CD1d and CEACAM5 depends upon the integrity of fragments 2 to 5 of the B3 domain. (Figure 6).

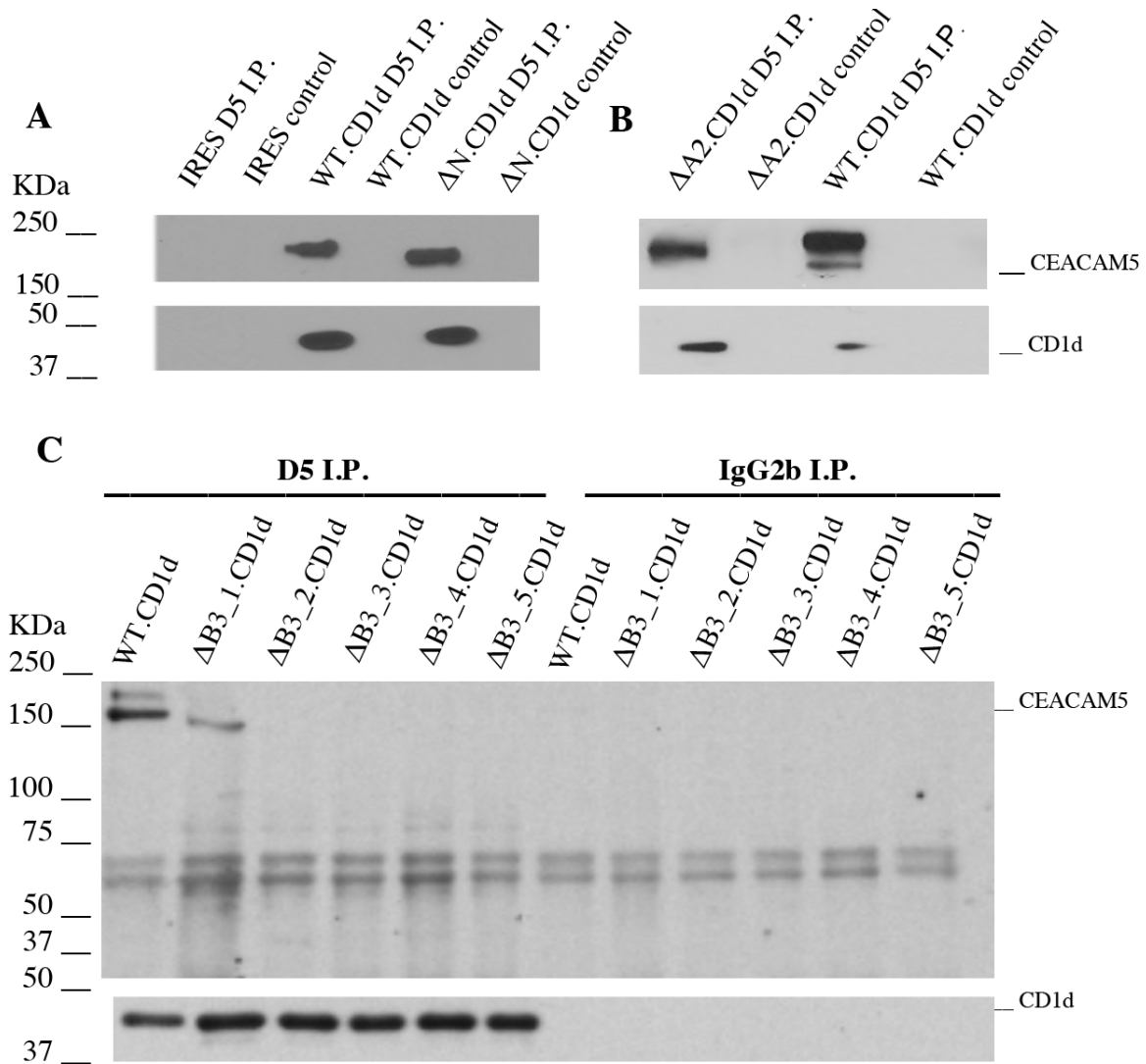


Figure 6. The B3 domain of CEACAM5 interacts with CD1d.

293T cells were transfected with expression vectors pCDNA3.1-IRES expressing CD1d and wild-type or truncated CEACAM5. The cell lysate of the transfectants was immunoprecipitated with mouse IgG2b anti-CD1d (D5). Western blot was then performed with Col-1 and D5 mAbs. (a,b) WT and CEACAM5 with the deletion of N-domain (N) co-immunoprecipitate with CD1d. WT and CEACAM5

with the deletion of A2-domain (A2) co-immunoprecipitate with CD1d. (c) CEACAM5 with the sequential C-terminal truncations of each domain fails to co-immunoprecipitate with CD1d. (d) CEACAM5 with the deletion of fragment 1 of B3-domain co-immunoprecipitates with CD1d. With further deletion of the B3 domain, CEACAM5 fails to co-immunoprecipitate with CD1d. Data are representative of three independent experiments.

CEACAM5 binds to CD8 α chains and induces CD8 associated kinase p56Lck phosphorylation

CEACAM5 exists as a glycosylphosphatidylinositol (GPI)-anchored glycoprotein on the surface of IECs. The molecule can therefore be removed by cleaving the anchor with the enzyme PIPLC as previously described (8). CEACAM5 released from transfected 293T cells by PIPLC treatment was used in a series of absorption studies. Murine T cell hybridoma transfectants expressing either human CD4 (3G4) or human CD8 α (3G8) were cultured with PIPLC supernatants from CEACAM5 or vector control 293T cell transfectants. Absorption of CEACAM5 from the supernatants by either CD4 or CD8 was determined by immunoblotting using mAb B9. Human CD8 α but not CD4 transfected hybridoma cells were capable of absorbing the B9 reactive material (Figure 7). These findings are consistent with functional properties previously ascribed to gp180. We next wanted to determine whether binding to CD8 had functional significance, evaluating CEACAM5's ability to induce CD8 associated kinase p56Lck. An anti-phosphotyrosine Western Blot revealed more pronounced phosphorylation of p56Lck from CEACAM5 and 3G8 co-incubation than from

CEACAM5 and 3G4 co-incubation. These data suggest that not only could CEACAM5 bind specifically to CD8 but also induce phosphorylation of CD8 associated p56Lck similar to the functional effect of gp180 (Figure 7).

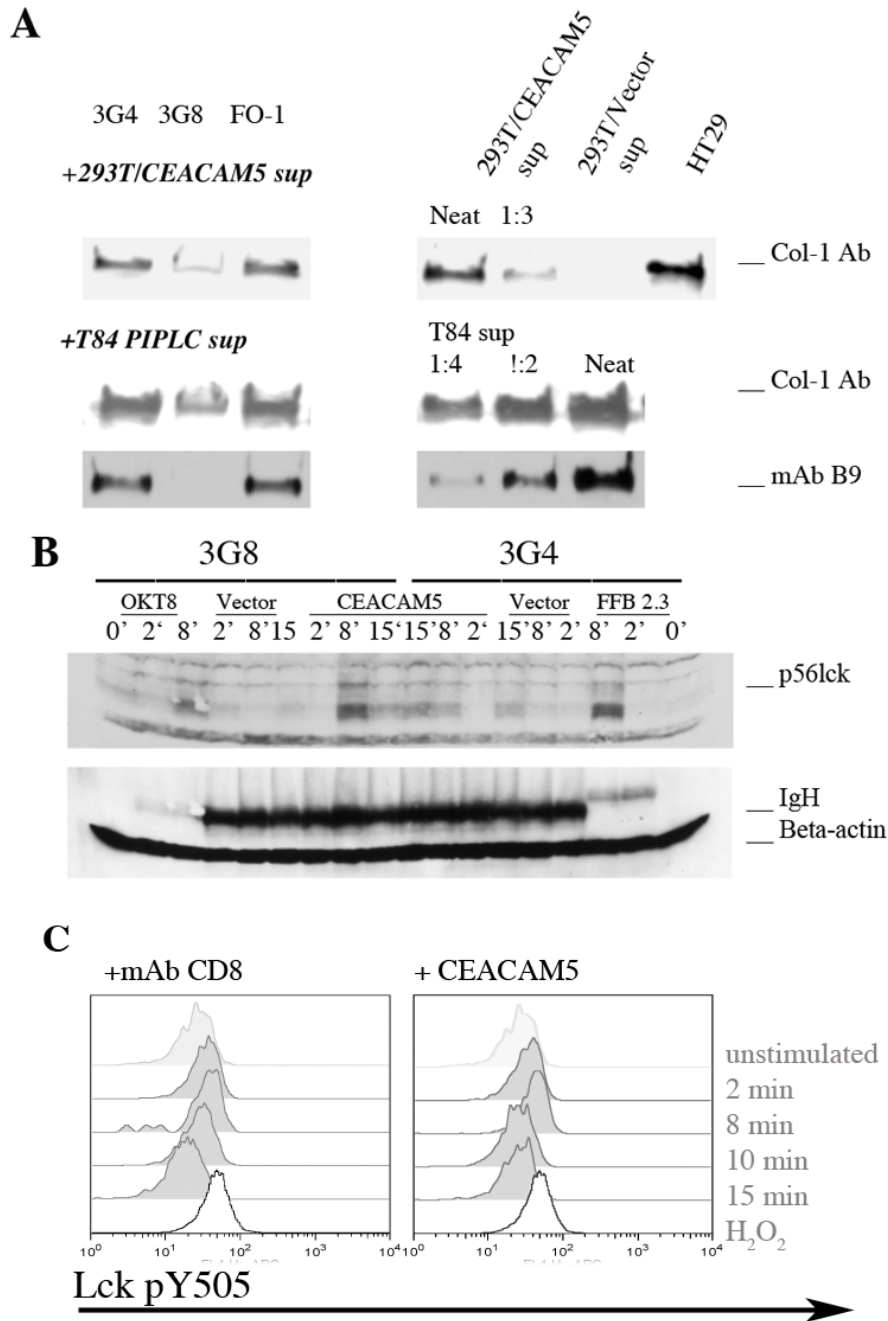


Figure 7

A. 3G4 and 3G8 cells were incubated with PIPLC supernatants from CEACAM5

transfectants, vector control 293 T cells, or IECs cell line T84. FO-1 cells were used as negative control. Absorbed or unabsorbed supernatants were subjected for immunoblotting using Col-1 or B9 mAbs. 3G8 but not 3G8 were capable of absorbing CEACAM5.

B. 3G4 and 3G8 cells were incubated with 293T/CEACAM5 or 293T/vector-PIPLC supernatants and subjected to immunoblotting for anti-phosphotyrosine mAb. OKT8 (anti-human CD8 antibody) and FFB2.3 (anti-human CD4 antibody) were used as positive controls. 3G8 cells incubated with CEACAM5 supernatants show more pronounced phosphorylation of p56Lck.

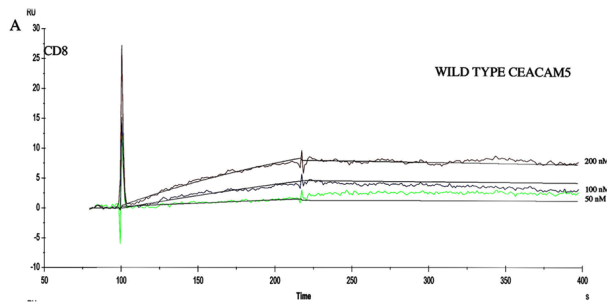
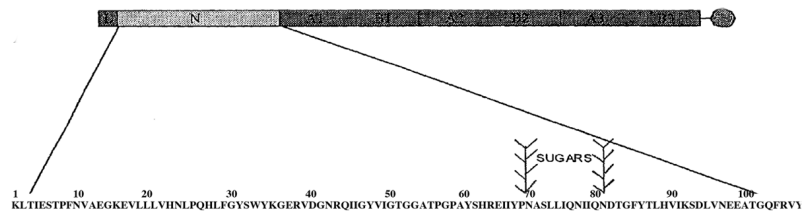
Biacore analysis of CEACAM5-CD8 α binding

Binding of wild type CEACAM5 and CD8 α was evaluated using Biacore. In this system, one molecule (in our case soluble ligand CD8 α or CD4 (as a control) is immobilized on a dextran matrix and the putative analyte is passed over the surface in solution (in our case CEACAM5 wild type or mutants). A full kinetic analysis of wild type CEACAM5/CD8 α binding revealed that CEACAM5 interacts with CD8 α with an equivalent affinity to CD8 α /MHC I interactions (Figure 8A) (30, 31). K_{on} is $2.60E+04$ M⁻¹s⁻¹ and K_{off} is $5.60E-04$ s⁻¹. The derived affinity constant is $2.20E-08$ M. Binding was observed at a 50 nM concentration of the wild type CEACAM5. No binding was observed between wild type CEACAM5 and a recombinant CD4 protein (Figure 8B). We next assessed whether the N⁴²RQII deletion of CEACAM5 affects binding to CD8 α . Biacore analysis showed a reduction in the KD when compared with the wild type (N⁴²RQII-

KD=1.70E-08 M; Kon=9E+04 M-1s-1; Koff=1.5E-03 s-1) (Figure 8C).

Subsequently we compared the affinity of wild type CEACAM5/CD8 α interactions with the CEACAM5 mutants. The affinity of N70,81A CEACAM5/CD8 α binding (KD=1.60E-05 M) appeared to be the lowest when compared to the wild type CEACAM5 with a lower Kon (2.90E+02 M-1s-1) and a lower Koff (4.70E-03 s-1). Similarly, the K35A KD was decreased (KD 1.50E-07 M) with a Kon of 1.50E+04 M-1s-1 and a Koff of 2.30E-03 s-1 (Figure 8C).

These results suggested that the loss of the glycosylation affects the conformational structure of CEACAM5, thus resulting in a reduction in affinity between CEACAM5/CD8.



		KD
WT CEACAM5	Full length	
N ⁴² RQII CEACAM5	Deletion of N42 to I46 disrupts the conformation	1.70E-08
K35A CEACAM5	Single point mutation	1.50E-07
N70,81A CEACAM5	Prevents N glycosylation	1.60E-05

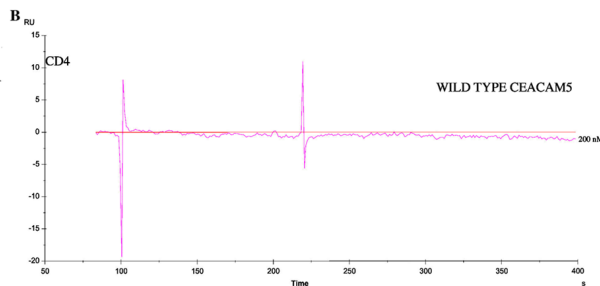


Figure 8

Binding of soluble wild type CEACAM5 (A) to immobilized CD8 α peptide and of wild type CEACAM5 to immobilized recombinant CD4 peptide (B). KD values of binding of WILD TYPE CEACAM5, N⁴²RQII, K35A and N70,81A to immobilized CD8 α peptide are shown in panel C.

mAb B9 blocks CEACAM5/CD8 binding

To finally demonstrate the partial overlap between mAb B9 and CD8 binding site on CEACAM5, we premixed CEACAM5 peptide with mAb B9 and consecutively added the mixture to CD8 α on the chip. As expected, no binding was observed (Figure 9).

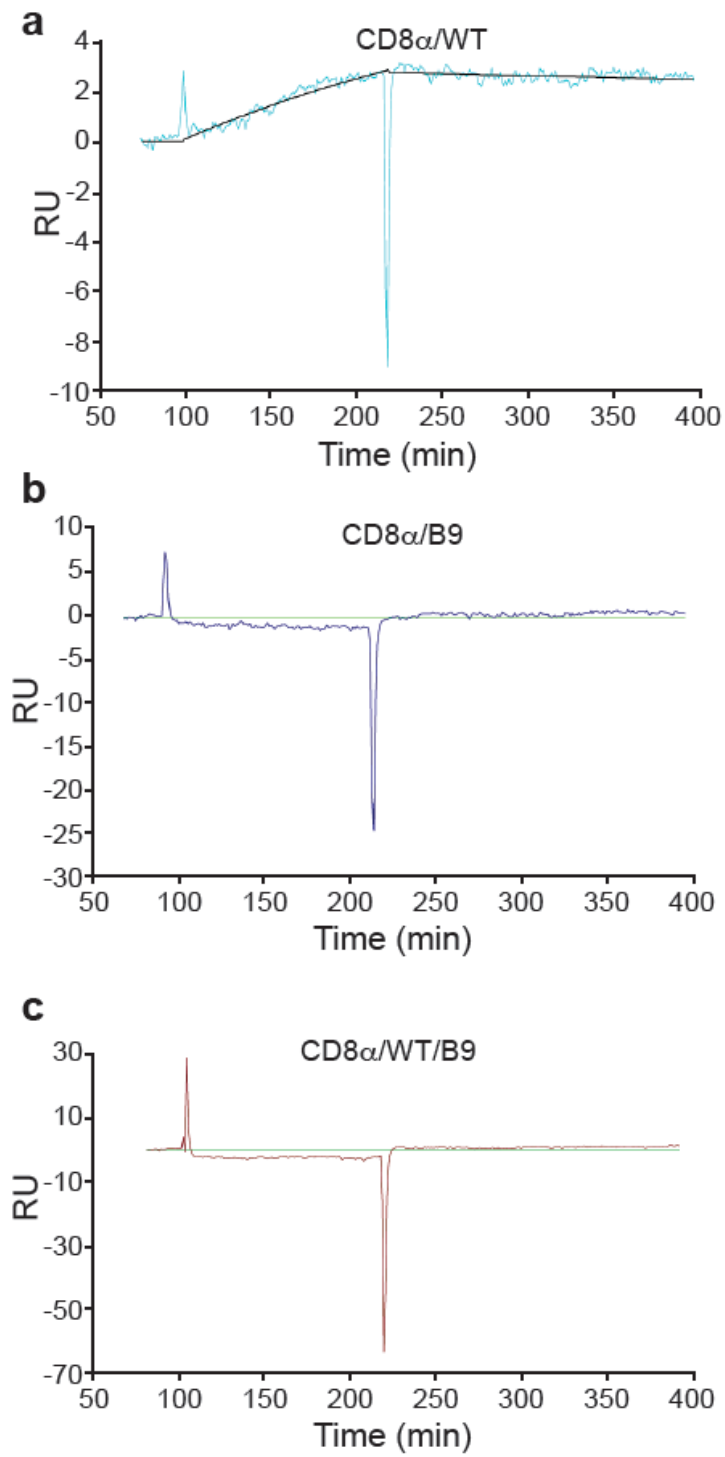


Figure 9. B9 blocks CEACAM5-CD8 α binding

(a) Binding of soluble WT CEACAM5 to immobilized CD8 α peptide. (b) Binding of B9 to immobilized CD8 α . (c) Binding of WT CEACAM5 premixed with mAb B9 (1:2) to immobilized CD8 α peptide.

2.5 DISCUSSION

Our previous studies have focused on a novel role for IECs as antigen presenting cells. In the normal state, IECs acts as non professional antigen presenting cells, such presentation results in the selective activation of CD8⁺ suppressor T cells. We have characterized this interaction by identifying two molecules expressed by normal IECs which bind to the T cell receptor (TCR) and CD8 molecules on these regulatory T cells, CD1d and gp180, respectively. We have also generated a monoclonal antibody that specifically recognizes gp180. We have determined that this mAb was epithelial cell specific; it inhibited IEC induced CD8⁺ T cell proliferation and blocked the activation of CD8-associated Lck. This approach has lead to the identification of molecules involved in IEC:T cell interactions, specifically CD8⁺ T cells. Purified gp180 was shown to be important in activating Lck through binding to CD8 α and CD1d (8-18).

All CEACAMs members have been shown to function, at least *in vitro*, as homotypic and heterotypic intercellular adhesion molecules. Modification in the expression of two GPI-anchored members, CEACAM5 and CEACAM6 have been shown to inhibit differentiation and anoikis, to disrupt cell polarization and tissue architecture, effects that altogether enhance tumorigenesis. CEACAM1 has been described to participate in the modulation of T cell function to bile acid

transport (19-29). More recently, CEACAM6 has been proposed as a receptor for the type 1 pili expressed by adherent-invasive Escherichia coli (AIEC) and its abnormal expression seen in Crohn's disease patients has been correlated to higher colonization and inflammation induced by AIEC (32).

In this study we described homology between gp180 and CEACAM5. We showed that CEACAM5 has properties of gp180 such as binding to CD8 α and induces Lck phosphorylation and interaction with CD1d. We confirmed that CEACAM5 interacts with CD1d through the B3-domain and that the sugar bridge between residues 70 and 81, which is the first highly conserved glycosylation site within the N-domain implicated in protein-protein interactions, is crucial for CEACAM5/CD8 binding and CD8 kinase Lck activation (26). Biacore protein-protein affinity analysis validated that the N70,81A mutant strongly impacts CEACAM5/CD8 binding. Therefore glycosylation of the N-domain of CEACAM5 is crucial for its interactions to CD8 α . Moreover, we have proven that B9 mAb and CD8 α have affinity to a similar binding site on CEACAM5 by competition experiments. These findings corroborate with previous observations and confirmed that B9 mAb blocks the induction of CD8⁺ regulatory T cells (Figure 9). We previously described that IECs derived from IBD patients have a defect in the expression of CEACAM5 (gp180) due to an evident failure to activate CD8⁺ regulatory T cells (33). Understanding the interactions between CEACAM5/CD1d and CD8 α /TCR in the mucosal immune system in normal individuals will allow the development of new approaches to promote induction of suppressive

immune responses (in Crohn's disease) or to enhance mucosal immunity (oral vaccines).

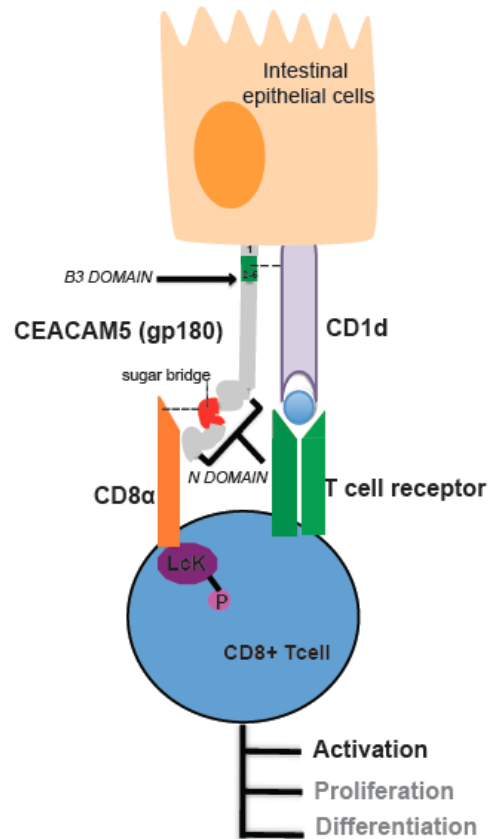


Figure 10. Interactions between CEACAM5/CD1d and CEACAM5/CD8α

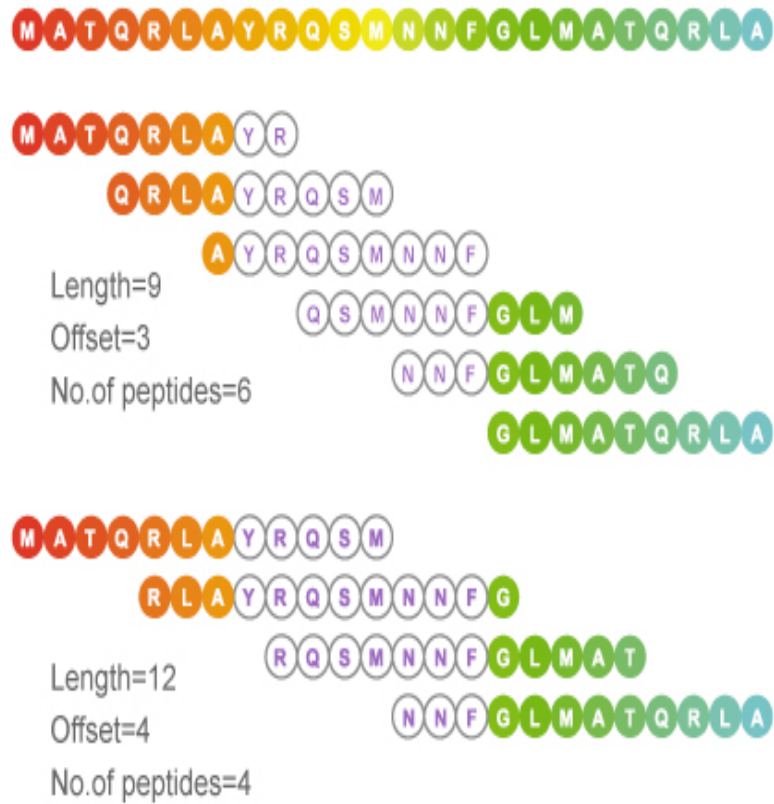
Intestinal epithelial cells express CEACAM5 and CD1d on their surface. CEACAM5 (gp180) interacts with CD1d through the B3 domain. Fragment 1 of the B3 domain is not required for its interaction with CEACAM5. The sugar bridge in the N domain of CEACAM5 is crucial for its binding to CD8α and for the activation of CD8-associated LcK (2).

3. Overlapping peptide library as a tool for the development of synthetic peptides to use as potential therapeutic agents.

3.1 Background

An overlapping peptide library is most commonly used for linear, continuous epitope mapping, where the aim is to generate a library of overlapping peptide sequences of specific length and specific offset, to cover a fragment or the entire native protein sequence. Characterized by two parameters, fragment length and offset number, each library is generated by breaking the original protein or peptide into many equal-length overlapping fragments, each has 8 to 20 residues. The offset number is the number of amino acid residues shifted between adjacent fragments and it reflects the degree of overlap. The offset number is usually chosen to be 1/3 of the fragment length. We generated a specific overlapping peptide library of the N domain of CEACAM5 to figure out which part contains the essential amino acids that contribute to its functionality.

Overlapping Library



3.2 METHODS

3.2.1 CEACAM5 overlapping peptide library

The N domain of CEACAM5 consists in 108 aminoacid residues. We generated a peptides library of 20 peptides each of 15 mer with an offset of 5. (JPT, Innovative Peptides Solutions, Germany).

Peptide n°	SEQUENCE
1	H-KLTIESTPFNVAEGK-OH
2	H-STPFNVAEGKEVLLL-OH
3	H-VAEGKEVLLL VHNL P-OH
4	H-EVLLL VHNL PQHLFG-OH
5	H-VHNL PQHLFGYSWYK-OH
6	H-QHLFGYSWYKGERVD-OH
7	H-YSWYKGERVDGNRQI-OH
8	H-GERVDGNRQIIGYVI-OH
9	H-GNRQIIGYVIGTQQA-OH
10	H-IGYVIGTQQATPGPA-OH
11	H-GTQQATPGPAYSGRE-OH
12	H-TPGPAYSGREIYPN-OH
13	H-YSGREIYPNASLLI-OH
14	H-IIYPNASLLIQNIIQ-OH
15	H-ASLLIQNIIQNDTGF-OH
16	H-QNIIQNDTGFYTLHV-OH
17	H-NDTGFYTLHVIKSDL-OH
18	H-YTLHVIKSDLVNEEA-OH
19	H-IKSDLVNEEATGQFR-OH
20	H-SDLVNEEATGQFRVY-OH

Table 3: CEACAM5's peptides library

3.2.2 Isolation of human CD8⁺ T cells

Peripheral blood mononuclear cells (PBMCs) were isolated from heparinized venous blood on a Ficoll-Hypaque density gradient (Amersham Biosciences, Piscataway, NJ) according to standard procedures. PB CD8⁺ T cells were isolated by negative selection using a human CD8⁺ T-cell Enrichment Kit (StemCell Technologies Inc, Vancouver, British Columbia, Canada).

3.2.3 In-Cell Western Blot

In order to assess the functionality of CEACAM5 N domain peptides library we used The In-Cell Western™ Assay that is an immunocytochemical assay that uses NIR fluorescence to detect and quantify proteins in fixed cells.

We selected 2 cells type to work with: 3G8 cell line and human isolated CD8⁺ T cells. Because the number of CD8⁺ T cells isolated from PBMC (peripheral blood mononuclear cells) is around 20% of total PBMC, the choice of this technique reduce the amount of cells needed for each condition.

200 X 10⁴ 3G8 or CD8⁺ T cells were seeded in a 96 flat wells plate and starved in RPMI serum free medium overnight at 37°C.

The day of the experiment the 96 plate was placed in ice for 15 minutes prior to perform the experiments.

We performed a series of experiments where cells were stimulated with OKT8 (10ug/mL) prior incubation with a IgG crosslinker for 15', cross linker alone,

H₂O₂ as positive control (0.8 μ M), purified CEACAM5 peptide (10 μ g/mL), N70,81A CEACAM5 purified mutant, pool of peptides or different combination of peptides for different time points (0, 2, 5, 10, 15 minutes). Unstimulated cells were obtained from each condition. A titration assay was performed with 1, 10, 100 μ g/ml of the pool of peptides to assess the optimal concentration of peptides to use to perform all the experiments.

Stimulation was stopped using a 4% formaldehyde buffer for 20 minutes followed by centrifugation for 10 minutes at 15000 rpm. Permeabilization was performed washing Cells with 1x PBS containing 0.1% Triton x-100 for 5 minutes per wash. After permeabilization cells were incubated for 1 hour with the blocking buffer (Odyssey Blocking buffer-LICOR) and then the primary antibodies goat anti-actin and rabbit anti pLcK were added overnight at 4°C. The day after cells were washed 5 times with 1x PBS+0.1% Tween 20 and incubated for 1 hour with the secondary antibodies (IRDye 800CW donkey anti goat IgG, IRDye 680 CW donkey anti rabbit IgG) for 1 hour at room temperature. Followed by 5 washes. Wells were dried and the plate was scanned using an Odyssey system. The software ImageStudio was used for quantification based on actin and background controls.

3. Peptides functionality evaluation: CD8-associated LcK phosphorylation

The titration assay revealed that 10 ug/mL of peptide is the concentration that mimic the kinetic of the purified CEACAM peptide.

The combination of 20 peptides that cover the entire N domain was capable of phosphorylated LcK in both 3G8 and human CD8+T cells at the same level as CEACAM5.

We then grouped the peptides in 3 different pool:

Pool1 to cover the aminoacid residues from 1 to 29,

Pool2 to cover the aminoacid residues from 30 to 66 and

Pool3 to cover the remaining aminoacids residues.

This order was determined in agreement with the previous data that have shown that the aa residues 70 and 81 are crucial for CEACAM5 functionality.

As expected, Pool 3 resulted in phosphorylation of LcK at a level comparable with the entire collection of peptides. On the contrary Pool 1 didn't give any results.

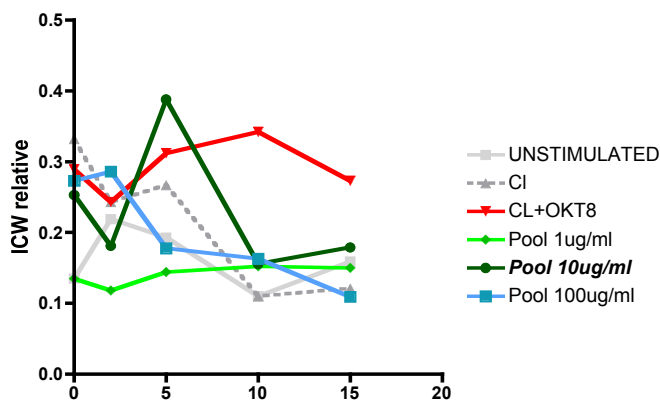
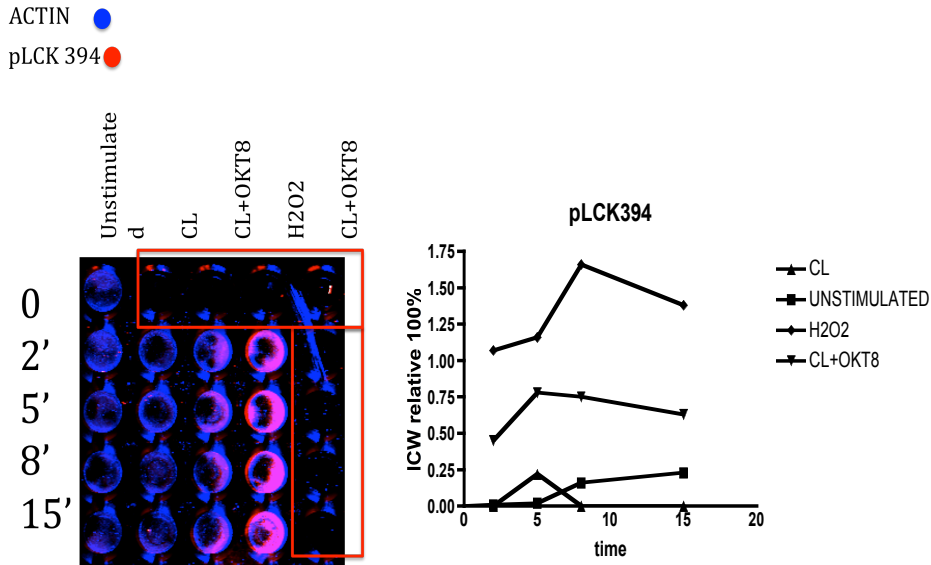


Figure 11: Tritation assay: 10ug/mL of the entire collection of peptides determines phosphorylation of Lck at a level comparable to OKT8.

A



B

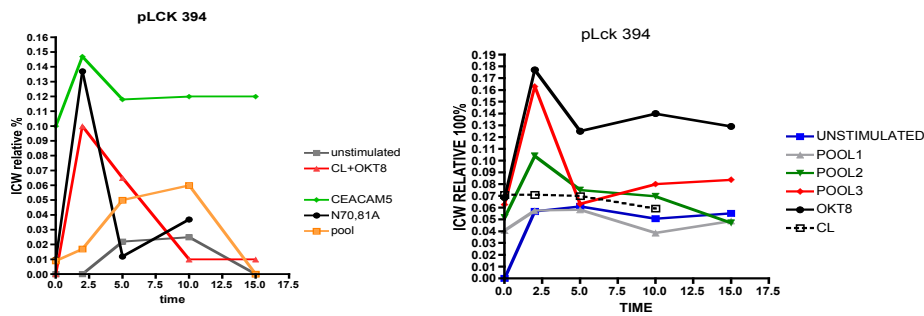


Figure 12: Phosphorylation of Lck in human isolated CD8+ T cells. A.

Representation of 1 of 3 In-cell Western Blot experiments where Human CD8+ T cells were cultured in presence of OKT8+/-cross linker and presence of H2O2 (positive control).

B. Left panel: CEACAM5 purified peptide induces phosphorylation of Lck as well as the entire collection of peptides. The N70, 81A purified peptide induce phosphorylation at 2' but the signal drop to the

unstimulated level. **Right panel:** Pool 3 determines phosphorylation in 2' at a level comparable with OKT8.

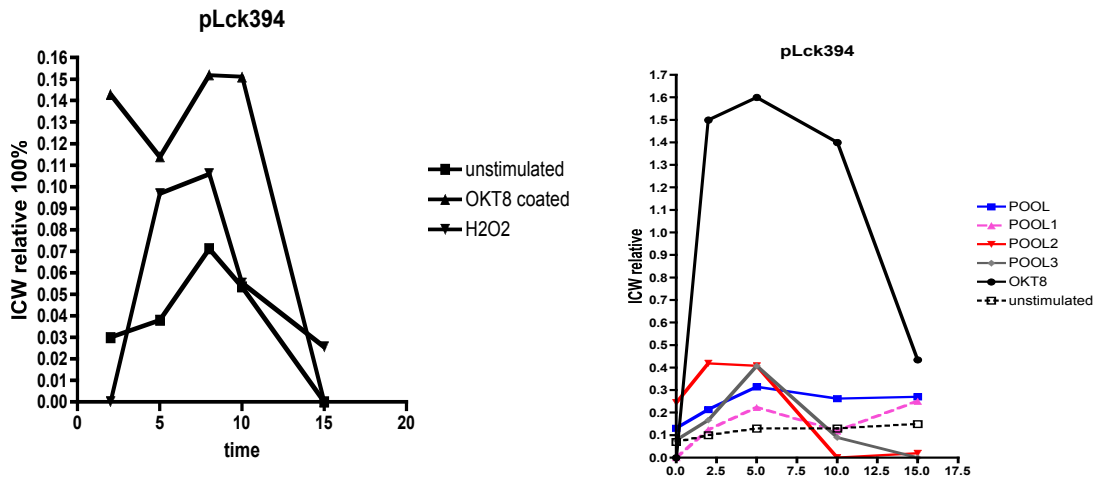


Figure 13: Phosphorylation of LcK in 3G8 cell line. Left panel: Representation of 1 of 3 In-cell Western Blot experiments where 3G8 were cultured in presence of OKT8+ coated on the plate overnight and presence of H2O2 (positive control). **Right panel:** The entire collection of peptides induce phosphorylation of Lck; Pool 3 determines phosphorylation in 2' at a level comparable with OKT8.

3.4 Conclusion

The CEACAM5 overlapping peptides library represents a tool to ascertain the epitope involved in CEACAM5 functionality. We have shown that we can create a collection of peptides without losing the capability of CEACAM5 to phosphorylate CD8-associated Lck.

Moreover we have already shown that the region where the residue N70 and N80 are located is crucial for CEACAM5 immunoregulatory function.

More experiments are required to test each peptide individually. Moreover we plan to understand whether the role of CEACAM5 is the one of activation of CD8 or it is a mechanism required for proliferation and differentiation. To address this question we will perform proliferation as well as suppression assay which will explain whether CEACAM5 is a trigger to induce a suppressive phenotype in normal homeostasis. Once, we will understand the whole role of CEACAM5 we will be able to use the peptides we generated in the development of new therapeutical strategy for the treatment of IBD.

REFERENCES

1. Bland, P.W. MHC class II expression by the gut epithelium. *Immunol. Today* **9**, 174–178 (1988).
2. Bland, P.W & Warren, L.G. Antigen presentation by epithelial cells of the rat small intestine. II. Selective induction of suppressor T cells. *Immunology* **58**, 9–14 (1986).
3. Bland, P.W. & Whiting, C.V. Antigen processing by isolated rat intestinal villus enterocytes. *Immunology* **68**, 497–502 (1989).
4. Hershberg, R. *et al.* Expression of the thymus leukemia antigen in mouse intestinal epithelium. *Proc. Natl. Acad. Sci.* **87**, 9727–9731 (1990).
5. Hershberg, R.M. *et al.* Intestinal epithelial cells use two distinct pathways for HLA class II antigen processing. *J. Clin. Invest.* **100**, 204–215 (1997).
6. Kaiserlian, D., Vidal, K. & Revillard, J.P. Murine enterocytes can present soluble antigen to specific class II restricted CD4+ T cells. *Eur. J. Immunol.* **19**, 1513–1516 (1989).
7. Mayer, L., So, L.P., Yio, X.Y. & Small, G. Antigen trafficking in the intestine. *Ann. NY Acad. Sci.* **778**, 28–35 (1996).
8. Yio, X.Y. & Mayer, L. Characterization of a 180-kDa intestinal epithelial cell membrane glycoprotein, gp180 A candidate molecule mediating t cell-epithelial cell interactions. *J Biol Chem* **272**, 12786–12792 (1997).
9. Campbell, N.A. *et al.* A Non-class I MHC Intestinal Epithelial Surface Glycoprotein, gp180, Binds to CD8. *Clinical Immunology* **102**, 267-274 (2002).

10. Allez, M., Brimnes, J., Dotan, I. & Mayer, L. Expansion of CD8+ T cells with regulatory function after interaction with intestinal epithelial cells. *Gastroenterology* **123**:1516–1526 (2002).
11. Allez, M., Brimnes, J., Shao, L., Dotan, I., Nakasawa, A. & Mayer, L.. Activation of a unique population of CD8(+) T cells by intestinal epithelial cells. *Ann N Y Acad Sci.* **1029**, 22–35 (2004).
12. Allez, M. & Mayer, L. Regulatory T cells: peace keepers in the gut. *Inflamm Bowel Dis* **10**, 666–676 (2004).
13. Arosa, F.A., Irwin, C., Mayer, L., de Sousa, M. & Posnett, D.N. Interactions between peripheral blood CD8 T lymphocytes and intestinal epithelial cells (IEC). *Clin Exp Immunol* **112**, 226–236 (1998).
14. Li, Y., Yio, X.Y. & Mayer, L. Human intestinal epithelial cell-induced CD8+ T cell activation is mediated through CD8 and the activation of CD8-associated p56Lck. *J Exp Med* **182**, 1079–1088 (1995).
15. Mayer, L. IBD: immunologic research at The Mount Sinai Hospital. *Mt Sinai J Med.* **67**, 208–213 (2000).
16. Somnay-Wadgaonkar, K. *et al.* Immunolocalization of CD1d in human intestinal epithelial cells and identification of a beta2-microglobulin-associated form. *Int Immunol.* **11**, 383–392 (1999).
17. Van de Wal, Y. *et al.* Delineation of a CD1d-restricted antigen presentation pathway associated with human and mouse intestinal epithelial cells. *Gastroenterology* **124** 1420–1431 (2003).
18. Toy, L.S., Yio, X.Y., Lin, A., Honing, S., Mayer, L. Defective expression of

- gp180, a novel. CD8 ligand on intestinal epithelial cells, in inflammatory bowel disease. *J Clin Invest* **100**, 2062–2071(1997).
19. Hammarström, S. The carcinoembryonic antigen (CEA) family: structures, suggested functions and expression in normal and malignant tissues. *Semin Cancer Biol* **9(2)**, 67-81 (1999).
20. Kinugasa, T. *et al.* Expression of four CEA family antigens (CEA, NCA, BGP and CGM2) in normal and cancerous gastric epithelial cells: up-regulation of BGP and CGM2 in carcinomas. *Int J Cancer* **30,76(1)**, 148-53 (1998).
21. Frangsmyr, L., Baranov, V. & Hammarstrom, S. Four carcinoembryonic antigen subfamily members, CEA, NCA, BGP and CGM2, selectively expressed in the normal human colonic epithelium, are integral components of the fuzzy coat. *Tumour Biol* **20**, 277–292 (1999).
22. Kuespert, K., Pils, S. & Hauck, C.R. CEACAMs: their role in physiology and pathophysiology. *Curr Opin Cell Biol* **18(5)**, 565-71 (2006).
23. Yan, Z. *et al.* Oncogenic c-Ki-ras but not oncogenic c-Ha-ras up-regulates CEA expression and disrupts basolateral polarity in colon epithelial cells. *J Biol Chem* **272**, 27902–27907 (1997).
24. Ordonez, C., Screatton, R.A., Ilantzis, C. & Stanners, C.P. Human carcinoembryonic antigen functions as a general inhibitor of anoikis. *Cancer Res.* **60**, 3419–3424 (2000).
25. Wirth, T., Soeth, E., Czubayko, F. & Juhl, H. Inhibition of endogenous carcinoembryonic in Crohn disease antigen (CEA) increases the apoptotic

- rate of colon cancer cells and inhibits metastatic tumor growth. *Clin Exp Metastasis* **19**, 155–160 (2002).
26. Bates PA, Luo J, Sternberg MJ. A predicted three-dimensional structure for the carcinoembryonic antigen (CEA). *FEBS Lett.* 1992;301(2):207-14.
27. Gangopadhyay, A., Lazure, D.A. & Thomas, P. Adhesion of colorectal carcinoma cells to the endothelium is mediated by cytokines from CEA stimulated Kupffer cells. *Clinical and Experimental Metastasis* **8**, 703-712 (1998).
28. Morales, V.M. *et al.* Regulation of human intestinal intraepithelial lymphocyte cytolytic function by biliary glycoprotein (CD66a). *J Immunol* **163(3)**, 1363-70 (1999).
29. Kammerer, R., Stober, D., Singer, B.B., Obrink, B. & Reimann, J. Carcinoembryonic antigen-related cell adhesion molecule 1 on murine dendritic cells is a potent regulator of T cell stimulation. *J. Immunol* **166**, 6537-44 (2001).
30. Huang, J., Lindsay, J., Evavold, B.D. & Cheng, Z. Kinetic of the MHC-CD8 interaction at the T cell membrane. *J Immunol* **179**, 7653-7662 (2007).
31. Jelonek, M.T., Classon, B.J., Hudson, P.J. & Margulies, D.H. Direct Binding of the MHC Class I Molecule H-2Ld to CD8: Interaction with the Amino Terminus of a Mature Cell Surface Protein. *The Journal of Immunology* **160**, 2809-2814 (1998).
32. Barnich, N. & Darfeuille-Michaud, A. Abnormal CEACAM6 expression patients favors gut colonization and inflammation by adherent-invasive E.

coli. Virulence **1(4)**, 281-2 (2010).

33. Roda, G. *et al.* Defect in CEACAM Family Member Expression in Crohn's Disease IECs Is Regulated by the Transcription Factor SOX9. *Inflamm Bowel Dis* **15(12)**, 1775-83 (2009).